

# **PRELIMINARY REGOLITH STUDIES AT EAREA DAM GOLD PROSPECT, GAWLER CRATON, SOUTH AUSTRALIA**

*M.J. Lintern*

**CRC LEME OPEN FILE REPORT 153**

**May 2004**

**(CSIRO Exploration and Mining Report 1150F)**

CRCLEME



# **PRELIMINARY REGOLITH STUDIES AT EAREA DAM GOLD PROSPECT, GAWLER CRATON, SOUTH AUSTRALIA**

*M.J. Lintern*

**CRC LEME OPEN FILE REPORT 153**

May 2004

(CSIRO Exploration and Mining Report 1150F)

© CRC LEME 2004

---

CRC LEME is an unincorporated joint venture between CSIRO-Exploration & Mining, and Land & Water, The Australian National University, Curtin University of Technology, University of Adelaide, Geoscience Australia, Primary Industries and Resources SA, NSW Department of Mineral Resources and Minerals Council of Australia.

*Headquarters:* CRC LEME c/o CSIRO Exploration and Mining, PO Box 1130, Bentley WA 6102, Australia

## © CRC LEME

This report presents outcomes of a collaborative research project between CRC LEME and the Department of Primary Industries and Resources, South Australia (PIRSA) that commenced in early and continued end 2002. It was agreed, between the parties, that this report could be released into the public domain immediately.

**Copies of this publication can be obtained from:**

The Publications Officer, CRC LEME, c/- CSIRO Exploration & Mining, PO Box 1130, Bentley WA 6102, Australia. Information on other publications in this series may be obtained from the above, or from <http://crcleme.org.au>

**Cataloguing-in-Publication:**

Lintern, M.J.

Preliminary regolith studies at Earea Dam Gold Prospect, Gawler Craton, South Australia

ISBN 0 643 06851 1

1. Regolith - South Australia 2. Landforms - South Australia 3. Geochemistry 4. Gold

I. Lintern, M.J. II. Title

CRC LEME Open File Report 153.

ISSN 1329-4768

**Address and affiliation of author:****M.J. Lintern**

Cooperative Research Centre for Landscape

Environments and Mineral Exploration

c/- CSIRO Exploration and Mining

PO Box 1130

Bentley WA 6102

Australia

© Cooperative Research Centre for  
Landscape Environments and Mineral Exploration  
2004

## PREFACE AND EXECUTIVE SUMMARY

This CRC LEME Open File Report describes preliminary regolith studies at the historic (*circa* 1899) Earea Dam Goldfield in the Gawler Craton, South Australia. The study was conducted as part of the PIRSA Harris Greenstone Project a pilot study for the PIRSA-CRC LEME Central Gawler Gold Province Project. Previous case studies of Au in the Gawler Craton regolith have been summarised in The South Australian Regolith Project (Lintern, 2004) and this case study complements these as it provides an example of Au dispersion in areas where regolith is relatively thin.

The Earea Dam Goldfield is located 34 km west of Kingoonya on the Tarcoola-Glendambo road. A regolith landform map at 1:20000 scale was constructed to set the geochemical study into context. Although the area has experienced mining activity, the particular location chosen to investigate geochemical dispersal of elements was not considered significantly disturbed. The prospect is located in rolling hills of 30-40 m relief on lapped by shallow alluvium-colluvium. Common bedrock exposures in the hills are Kenella Gneiss and scarcer intrusions of mafic dykes. The hills are mantled with fine to cobbled-sized lag of angular bedrock. Elsewhere, bedrock and saprolite are mostly covered by a fine-grained red-brown soil partly of aeolian origin. Observations of costeans, pits and limited drill spoil indicate that the depth of weathering is limited to a few metres in much of the area. Calcrete is common in the erosional regime but its extent beneath, and within, the hardpanized (silicified) colluvium-alluvium was not determined. The thickness of transported cover varies from outcrop to 3 m in the vicinity of the mineralization. Sand dunes and playas to the south and east serve to mask the underlying regolith.

The distribution of gold and other elements was investigated within a part of the Earea Dam Goldfield known as Ian's Mine (499444E 6585077N, AGD66), a 5 m by 20 m by 4 m deep mining slot with high grade ore hosted by quartz-hematite. Samples were taken from the slot and adjacent costeans, with a limited soil and auger survey downslope of the mineralization, followed by multi-element analyses.

Gold mineralization is associated with Ag, Bi, Cu, Sn, Te, U and W at Ian's Mine. In the immediate vicinity, surficial dispersion is mostly mechanical, associated with mineralized bedrock fragments. Some high concentrations of Au are recorded in calcrete (maximum of 475 ppb) largely due to included detrital hematite-quartz fragments. Some chemical processes may have led to limited dispersion of Au in smectitic clays adjacent to the mineralized quartz-hematite veins. By 200 m downslope of Ian's Mine, soil samples are close to background Au concentrations (2-3 ppb). Silver, and possibly W, are more widely dispersed than Au. Fine (<75  $\mu$ m) and coarse (>2 mm) size fractions are generally richer in Au and pathfinders than intermediate size fractions for material from Ian's Mine itself but only the fine fraction is richer in Au for soil from the depositional regime downslope of the mine. Calcrete has shown to be concentrated in Au in the erosional areas but its poor development in the surficial soils of the depositional areas precludes its use as a sampling medium in these areas.

In this environment, high-grade mineralization produces a limited geochemical dispersion halo for Au. Poorly-developed supergene Au, possibly due to the absence of a significant thickness of regolith within which it can develop, a resistant host rock (hematite-quartz), and the small, narrow characteristics of the veins may be possible explanations. Greater thicknesses of regolith, (with possible supergene redistribution) may have been present but have since been eroded. Exploring for more ore shoots of this type is expected to be difficult in this area unless very close spaced calcrete sampling (25 m grid) and/or transported-in situ interface sampling is adopted.

M.J. Lintern

Study Leader  
May 2004

# CONTENTS




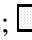
1	INTRODUCTION.....	1
1.1	Background .....	1
1.2	General work objectives.....	4
1.3	Specific work program .....	4
1.4	Location and access.....	4
1.5	Physiography.....	4
1.6	Historical data. ....	5
2	METHODS .....	5
2.1	Sample collection .....	5
2.2	Sample preparation and analyses .....	5
3	REGOLITH.....	6
3.1	Regolith stratigraphy .....	6
3.1.1	Overview .....	6
3.1.2	Basement (in situ).....	7
3.1.3	Saprolite .....	8
3.1.4	Hardpan .....	8
3.1.5	Dune sand.....	9
3.1.6	Calcrete.....	10
3.1.7	Soils.....	12
3.2	Regolith-landforms.....	12
3.2.1	Introduction and methods.....	12
3.2.2	Regolith-landforms.....	12
4	GEOCHEMISTRY.....	16
4.1	Introduction .....	16
4.2	Mineralogy .....	16
4.3	Mineralization .....	17
4.4	South wall of pit .....	19
4.5	Eastern wall of pit geochemistry .....	24
4.6	Northern wall of pit geochemistry.....	24
4.7	Soil geochemistry .....	29
4.8	SIZE FRACTION ANALYSIS.....	37
5	CONCLUSIONS.....	40
6	IMPLICATIONS FOR EXPLORATION .....	40
7	SUMMARY .....	40
8	ACKNOWLEDGEMENTS .....	40
9	REFERENCES.....	41
10	APPENDICES.....	41

## LIST OF FIGURES

Figure 1: Map of the regional terrains of the Gawler Craton showing location of Earea Dam. The Harris Greenstone Belt terrain is coloured dark green and occurs near the centre of the Gawler Craton. (From PIRSA). .....	2
Figure 2: Location of Earea Dam Gold Prospect. Boxed area indicates approximate regolith-landform map boundaries (Figure 9). Colours used as a guide only to the age of geological units. For full explanation see GIS in Appendix. ....	3
Figure 3: Local geology, mining activity (including location of Ian's Mine) and boundary of the geochemical study described in this report. Modified after Crettenden and Fradd (1992). ....	3
Figure 4: Geology of the Earea Dam Prospect (Source: PIRSA GIS). ....	7
Figure 5: Bedrock occurrences at Earea Dam: 1) outcrop exposure on the edge of a clay pan; 2) lag of angular granitic material; 3) exposure of bedrock in small pit; 4) fresh bedrock within weathered material exposed in pit face at Ian's Mine. ....	8
Figure 6: 1) hardpan exposed in costean (see also photo 6 in Figure 8 to see context); 2) hardpan material showing dark purple Mn coatings. ....	9
Figure 7: Dune sands at Earea Dam: 1) southerly view from hill located to east of Ian's Mine with playa (distance) bordered by vegetated sand dunes (arrowed); 2) gypseous sand dune bordering playa. ....	9
Figure 8: Samples and field occurrence of calcrete: 1) sample ED114; 2) sample ED231; 3) sample ED21; 4) sample ED93; 5) sample ED21-1, comprised of granulite clast partly encased by calcrete; 6) costean partly located in depositional terrain showing calcrete on partings of hardpan; 7) laminar and massive calcrete in pit face of Ian's Mine; 8) costean showing calcrete coatings on mafic dyke saprock. ....	11
Figure 9: Regolith-landform map of the Earea Dam Prospect showing location of observation points (open circles), Ian's Mine and geochemical study area. The regolith map forms part of the GIS (Appendix data disc). For full regolith-landform description see text. ....	14
Figure 10: a) aerial photography, b) Landsat TM composite ratio image (bands 5/7, 4/7 and 4/2), c) ASTER bands 3, 2 and 1 (decorrelated stretch) and .....	15
Figure 11: Location plan of profiles sampled at Ian's Mine. The east face is about 4 m deep. ....	16
Figure 12: Bar charts showing concentration of selected elements in grab samples from Ian's Mine at Earea Dam Prospect. Samples are ranked (left to right) according to increasing Au content. Cadmium data are below 0.5 ppb. Sample numbers are indicated on the larger histogram. ....	18
Figure 13: SEM photomicrograph of hematite within quartz containing a 20-30 $\mu\text{m}$ Au grain (arrowed, and with <1% Ag) and "shards" of a Bi oxide. Other Bi minerals found contained Ba and/or V. ....	19
Figure 14: View of south face (Ian's Mine) in foreground with valley and dunes in background. Fifteen profiles were sampled from the south face and the geochemical data are contoured in Figure 15. The vehicle is parked in the western part of the pit facing the access ramp. ....	20
Figure 15: Distribution of selected elements in the southern pit wall of Ian's Mine. ....	21
Figure 16: Sample ID and distribution of selected elements in the eastern pit wall of Ian's Mine. ....	25
Figure 17: Distribution of selected elements in the northern pit wall of Ian's Mine. ....	27
Figure 18: Gold in soils: a) histogram of Au data. Lower soil samples are from variable depth between 20-160 cm; b) distribution of soil Au using maximum values at each location; c) Au vs. Ca scatter plot. ....	29
Figure 22: Calcium in soils: a) histogram of Ca data; b) distribution of soil Ca using maximum values at each location; c) Ca vs Cu-CN scatter plot. ....	31
Figure 23: Copper in soils: a) histograms of Cu data; b) distributions of soil Cu using maximum values at each location; c) Cu vs Cu-cn and Cu-cn vs Mg scatter plots. ....	32
Figure 32: Size fraction analysis (<75 $\mu\text{m}$ to >2000 $\mu\text{m}$ ) for 5 selected samples: ED21 – calcrete containing rock fragments (partially weathered pyroxene-hornblende granulite and granitoids); ED93 – friable nodular calcrete with rock fragments; ED114 – laminar and platy calcrete containing rock fragments; ED231 – friable, platy and nodular calcrete containing rock	

fragments; ED269 – clay-rich red soil from valley floor. The calcrete samples can be viewed in Figure 8. ....	38
Figure 33: Distribution of selected major and trace elements in size fractions (<75 µm to 2000 µm) of sample ED269. ....	38
Figure 34: Selected elemental distribution in three size fractions (<75 µm, 75-180 µm and >2000 µm) for samples ED114, ED21, ED231 and ED93. ....	39

## LIST OF TABLES

Table 1: Regolith-landform code, regolith type and description of units at Earea Dam Gold Prospect. ....	13
Table 2: Regolith landform unit, RTMAP code, number of occurrences (count), total area and % occurrence for the Earea Dam Gold Prospect. Units are ranked in order of % occurrence. ....	13
Table 3: Selected mineralogy of 4 profiles from Ian’s Mine, Earea Dam. Estimates of mineral abundances were based on peak height:  abundant;  moderately abundant;  some;  trace. See Figure 11 for location of samples, Figure 15 for geochemistry and location (Profile D) of samples ED01 to ED11, Figure 16 for geochemistry and location of samples ED12-30 and Figure 17 for geochemistry and location of samples ED31-45. ....	17
Table 4: Summary of elemental association and interpretation in south face of Ian’s Mine. ....	20

# **PRELIMINARY REGOLITH STUDIES AT EAREA DAM GOLD PROSPECT, GAWLER CRATON, SOUTH AUSTRALIA.**

M.J. Lintern

## **1 INTRODUCTION**

### **1.1 Background**

The Gawler Craton occupies almost half of South Australia, comprising deeply weathered Archaean and Proterozoic rocks covered by Mesozoic to Cainozoic sedimentary cover sequences. The Craton has been subdivided into 14 Domains, based on tectonic and lithotype criteria by Primary Industries and Resources South Australia (PIRSA). In the early 1990's Archaean komatiitic greenstones were discovered near Lake Harris, ESE of Tarcoola, during a South Australian Geological Survey-sponsored diamond drilling program. Airborne magnetic surveys have shown over 130 km of strike length and the area enclosing these greenstones has been designated the 'Harris Greenstone Domain' (Figure 1). Between 2000-2003, CRC LEME and the PIRSA Mineral Resources Group – Gawler Craton Team have provided exploration companies with data on lithotypes, geochemistry, structure, regolith characteristics, geochemistry and mineralization models so as to encourage further exploration in this area. Research on the weathering profile component was conducted under the “umbrella” of the Harris Greenstone Belt Regolith Project.

Little is known of (i) the weathering characteristics of greenstones in the Gawler Craton, (ii) their geochemical dispersal patterns related to weathering, (iii) their rock-mineral volume changes, or (iv) the hydrogeochemical or mechanical transport that any released elements of economic interest (Ni, PGE and Au) might have followed. Much of the greenstone strike length lies under shallow to moderate transported cover, ranging from Quaternary dune sands, thicker marine shales of the Mesozoic and perhaps some Permian Glacials.

The aim of the research, through the Targeted Exploration Initiative South Australia (TEISA) funding program, is to build on the expertise in weathering of greenstones from the Yilgarn Craton, from CSIRO Exploration and Mining and CRC LEME 1, to develop an understanding of greenstone equivalents in South Australia. The Harris Greenstone Domain is a 'greenfields area' requiring new research on regolith characterisation, regolith geochemistry and landscape evolution.

Aims of the regolith research are to:

- Characterize the weathered zones, both mineralogically and geochemically, within the greenstone and granitic-metasediment host rock sequences, produce a regolith map (selected strip-blocks at 1:5,000 & 1:10,000) both where out-subcropping as well as where overlain by thin to moderate transported cover.
- Combine this into a GIS database to assist mineral exploration, highlighting field sample methodologies, sample media and pathfinder element data sets most likely to vector to hidden primary mineralization.
- Enhance exploration for Ni, PGE and Au within this recently discovered greenstone terrain.

This particular study describes preliminary regolith studies on the distribution of Au and potential pathfinders at the Earea Dam Goldfield (Figure 2) which is located within granitoids adjacent to the greenstone sequence.



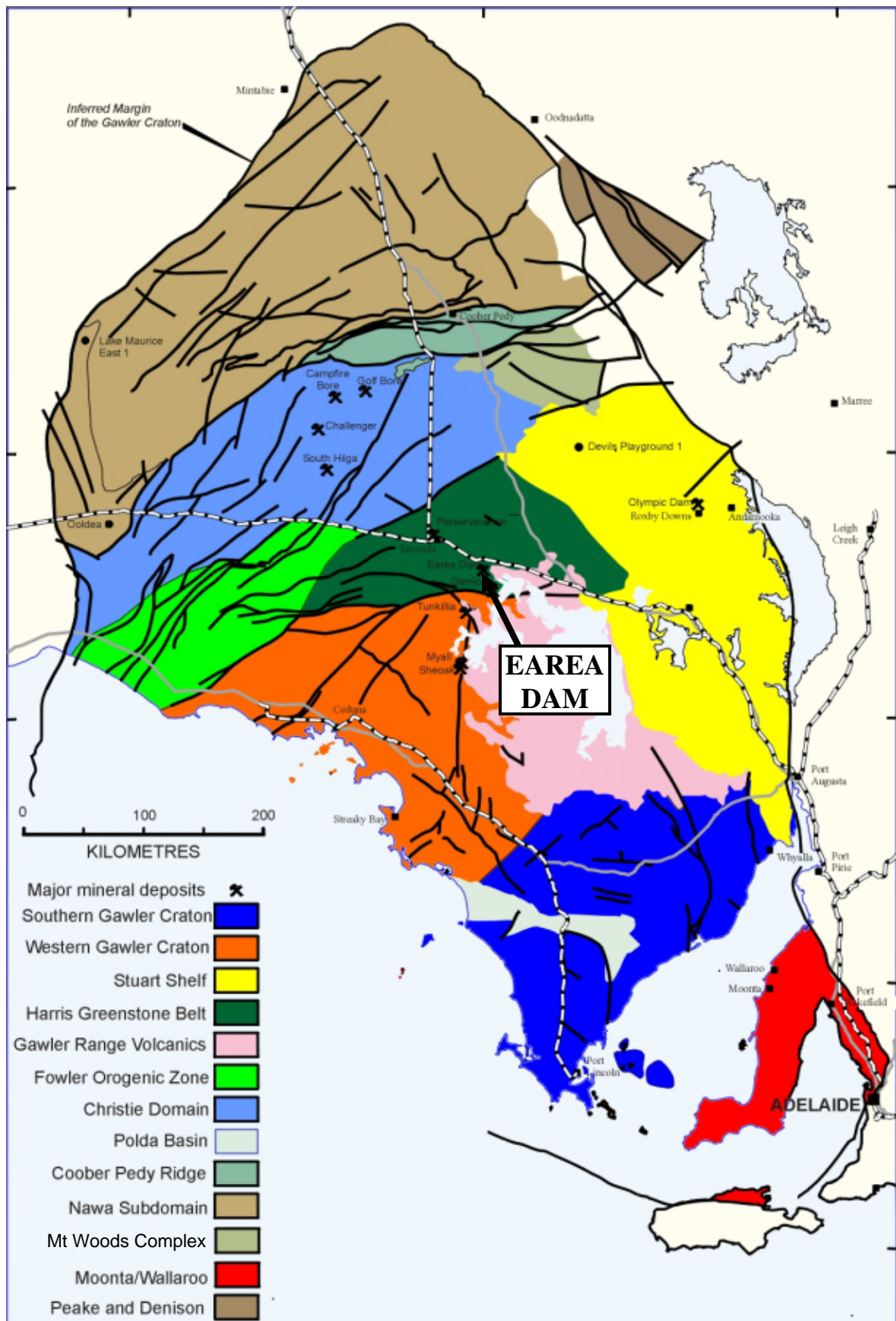


Figure 1: Map of the regional terrains of the Gawler Craton showing location of Earea Dam. The Harris Greenstone Belt terrain is coloured dark green and occurs near the centre of the Gawler Craton. (From PIRSA).

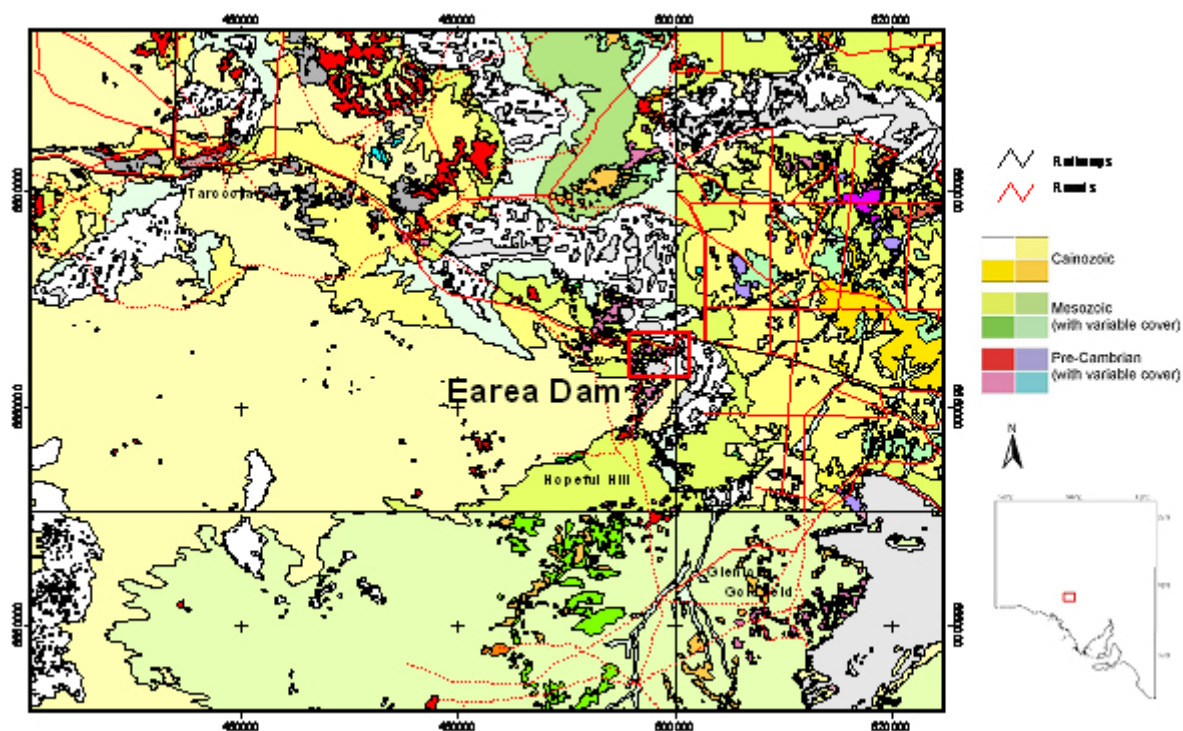


Figure 1: Location of Earea Dam Gold Prospect. Boxed area indicates approximate regolith-landform map boundaries (Figure 9). Colours used as a guide only to the age of geological units. For full explanation see GIS in Appendix.

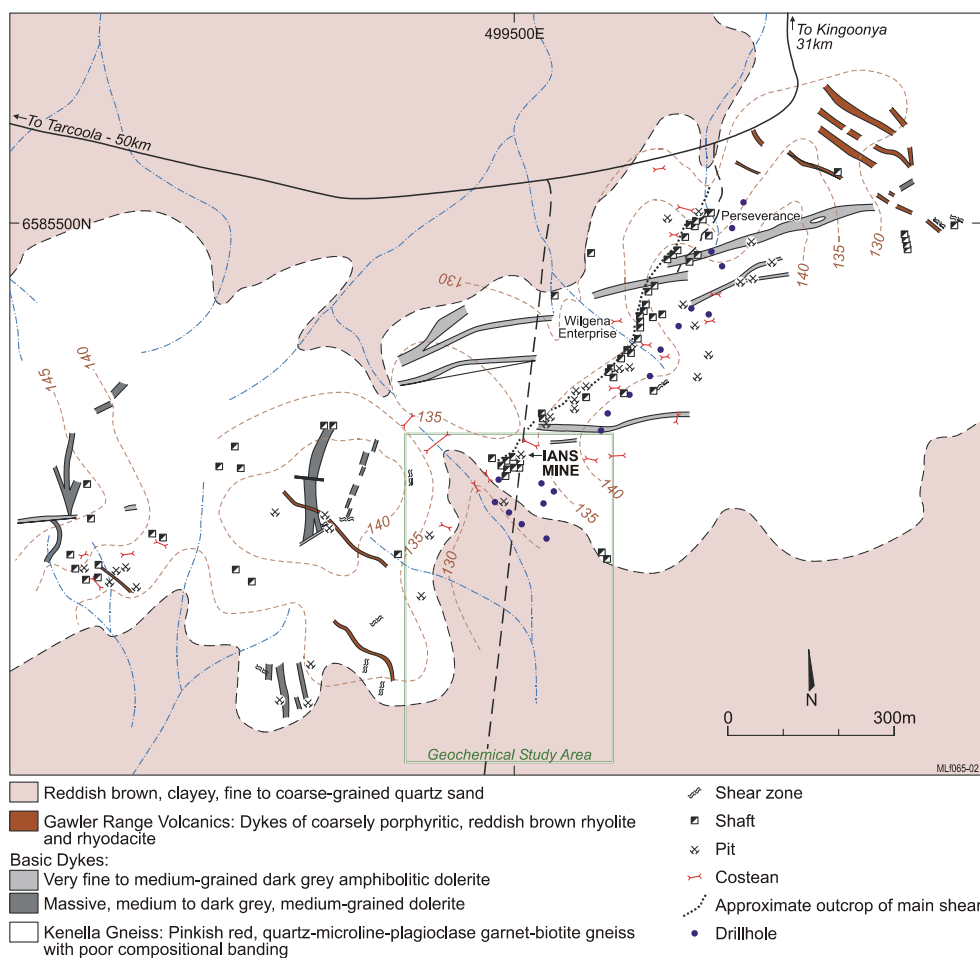


Figure 2: Local geology, mining activity (including location of Ian's Mine) and boundary of the geochemical study described in this report. Modified after Crettenden and Fradd (1992).

## 1.2 General work objectives

The primary objective of the Harris Greenstone Belt Project is “to characterise regolith (including sedimentary cover) over the recently discovered komatiitic greenstones within the Harris Greenstone Domain of the Gawler Craton”. Specific objectives are to:

- 1) Characterise the geochemical signatures and dispersal patterns at representative sites, then develop exploration methodologies, best sampling media and significant pathfinder element groupings.
- 2) Map carefully selected areas in detail (1:5,000 to 1:10,000) and model these, where possible, in 3D using additional information from drilling and other data.
- 3) Compare the SA greenstone regolith with those of the Yilgarn greenstone belts.
- 4) Promote findings to exploration industry.

The study at Earea Dam is located outside of the greenstone sequence but within the Harris Greenstone Domain and, therefore, specific object 1) above was not applied here.

## 1.3 Specific work program

1. Visit Earea Dam Prospect for preliminary reconnaissance in November 2001.
2. Visit Earea Dam Prospect in April 2002. Collect samples from Ian’s Mine and environs, and map regolith landforms.
3. Analyse samples for elemental concentrations, mineralogy and petrology and determine follow-up sampling program.
4. Re-visit Earea Dam Prospect in July 2002. Collect further samples to better determine extent of geochemical dispersion. Use powered auger to sample deeper in soil profile and attempt to target calcrete horizon (if present).
5. Analyse new samples.
6. Interpret data. Write report and present results.

## 1.4 Location and access

Earea Dam Prospect is located 550 km NW of Adelaide and 34 km west of Kingoonya at 499444E 6585077N (WGS84, UTM). Access is via a track running south for 0.5 km from the Glendambo to Tarcoola road. Tracks and roads are closed after heavy rain.

## 1.5 Physiography

The Earea Dam Prospect is situated amongst rolling hills with landforms characterised by gentle crests, simple gently- to moderately-inclined slopes to co-alluvium-dominated plains. Relief is 30-40 m. The geochemical study was conducted in a very gently sloping valley, 100 m wide at its head broadening to >300 m to the south, and 600 m long; the valley is bounded to the N, E and W by hills of partly weathered granitoid rocks, and by sand dunes to the south.

The nearest weather station is located at Tarcoola, 43 km to the WNW. The area is semi-arid and has sporadic rain falling during hot summers and mild to warm winters. Heavy rainfall can occur during winter, associated with cold fronts from the SW, or during summer, associated with rain-bearing depressions from cyclones originating in the NW. Mean daily maximum temperature, mean daily minimum temperature, highest maximum temperature and lowest minimum temperature are 27°C, 11°C, 49°C and -5°C, respectively. The mean annual rainfall and highest daily rainfall are 173 mm and 141 mm (during February), respectively. Climate data are courtesy of the Bureau of Meteorology.

Vegetation density and type is variable. In low lying areas open chenopod shrubland is the dominant formation consisting predominantly of *Maireana* and *Atriplex* spp. less than a metre high. The sand dunes are open low woodland of dominantly *Acacia* spp. The slopes and crests have a variety of vegetation forms including sparse shrubland, isolated shrubs and an understorey of open chenopod shrubland. Isolated trees of *Casuarina* spp., *Acacia* spp and *Alectryon oleifolius* occur throughout the study area.

## 1.6 Historical data.

Gold was first discovered at Earea Dam in 1899 in an outcrop of “magnetic iron ore and quartz” (Brown, 1908). Total recorded production from the field was 59.2 kg of Au from 1870 tonnes of ore. It was intermittently mined until the 1940s. Ore was transported off site, initially to Tarcoola and Glenloth batteries and later to Peterborough and Mt Torrens government batteries.

Mineralization is mostly restricted to a narrow shear zone with a 25-40 degree E-ESE dip and a 600 m strike length (Figure 3). The shear zone has cross cutting dykes, gneiss and granulite. Gold is associated with both vein quartz and hematitic material within the shear zone (Brown, 1908; Circosta and Gum, 1989) and is also visible in the gneiss. Drilling and rock-chip sampling by the SA Geological Survey returned values of 1.46 and 0.09 ppm Au from the dolerite dykes occurring close to the shear (Crettenden and Fradd, 1992).

After the 1988 SA Geological Survey (SADME) drilling program, Tarcoola Gold Ltd undertook follow-up geochemical and geophysical work (Circosta and Gum, 1989). One mineralized sample (>10 ppm Au) of dark hematitic material from Earea Dam was submitted for multi-element analysis. The following elements and concentrations were reported in ppm: Ag (1), As (24), Bi (290), Cu (530), Ni (24), Mo (3), Pb (32), Sb (14), Se (<2), Sn (48), Te (35), U (<4) and Zn (30). This type of element enrichment suggests a hydrothermal origin for the mineralization. In particular, the high concentrations of the chalcophiles Bi, Sb, and As indicate a low temperature sulphide association, although no S data were available to confirm this. Fluid inclusion studies of a quartz vein sample from the shear identified a CO<sub>2</sub>-rich fluid of moderate salinity and high gas content, with very high homogenisation temperatures (<500°C), supporting a hydrothermal origin of the mineralization (Crettenden and Fradd, 1992).

## 2 METHODS

### 2.1 Sample collection

Surficial soils were collected from 0-10 cm and 10-20 cm in shallow pits. Deeper soil samples were obtained either by accessing costeans or pits. Composite soil samples were obtained using a power auger. The thickness of the composite soil was dependent on the ability of the power auger to penetrate the regolith, particularly hardpan and saprolite (maximum of 1.6 m).

Detailed profile sampling focussed on an area called Ian's Mine (Figure 3). Soil, calcrete and saprolite samples were accessed from a shallow pit (~4 m deep, 5-12 m wide and 25 m long) using a ladder. Sample sites were photographed prior to collection to show their relative location and nature of the regolith material prior to disturbance.

### 2.2 Sample preparation and analyses

All samples were transferred to the CSIRO Sample Preparation Laboratory for sorting, drying and splitting. Samples were split by weighing, mixing the sample on a plastic sheet, and then incrementally extracting approximately 500 g of material (or about 50%, whichever was the smaller). Samples were tested for carbonate content with dilute acid (1M HCl).

Well-characterised in-house standards were entered into the analytical stream at approximately 1 per 30 samples to check for analytical precision and accuracy. All samples and standards were analysed by Ultra Trace Pty Ltd as follows (detection limits in ppm):

- (i) approximately 0.3 g of sample was analysed after a four acid digest (HF+HCl+HClO<sub>4</sub>+HNO<sub>3</sub>) by either (a) ICP-OES for Al (100), Ba (1), Ca (100), Co (2), Cu (1), K (20), Mn (1), Ni (1), V (2) and Zn (1) or (b) ICP-MS for Ag (0.5), As (0.5), Bi (0.1), Cd (0.5), Mo (0.2), Pb (1), Rb (0.02), Sb (0.2), Sn (1), Te (0.2), Tl (0.1), U (0.05) and W (0.5);
- (ii) approximately 0.25 g of sample was fused with Na<sub>2</sub>O<sub>2</sub>. The fused material is dissolved in HCl dilute to volume and analysed by either (a) ICP-OES for Cr (50), Fe (100), Mg (100), Si (100) and Ti (100) or (b) ICP-MS for Ce (0.5), Dy (0.5), Er (0.5), Eu (0.2), Gd (2), Ho (0.2), La (0.5), Lu (0.2), Nd (0.5), Pr (0.2), Sm (0.5), Sn (10), Tb (0.2), Tm (0.2), Yb (0.5) and Zr (10).

(iii) a 2 g sample was shaken with a 1000 ppm cyanide solution for 24 hour leach and analysed by ICP-MS for Au (0.0001), Ag (0.001) and Cu (0.05).

X-Ray diffraction of selected samples was undertaken at the ARRC Laboratories (CSIRO, Kensington, WA) using a Philips PW1050 diffractometer, fitted with a graphite crystal diffracted beam monochromator. CuK $\alpha$  radiation was used. Each sample was scanned over the range 2–65° 2 $\theta$  at a speed of 1° 2 $\theta$  per minute and data were collected at 0.02°2 $\theta$  intervals. Mineralogical compositions were determined by comparison with JCPDS files and laboratory standard traces.

A limited suite of SWIR spectra from soils were collected using an Analytical Spectral Device (ASD) Field SpecPro spectroradiometer. These are located in the Appendix.

### **3 REGOLITH**

#### **3.1 Regolith stratigraphy**

##### **3.1.1 Overview**

The principal original rock types of the erosional regime are Kenella Gneiss and intrusions of mafic dykes (Figure 4). Gneiss bedrock common outcrops on hill tops, hill slopes and in creek lines but, elsewhere, are mostly covered by a fine-grained red-brown soil partly of aeolian origin. The hills are littered with a fine to coarse lag mostly comprising of cobbles of angular bedrock.

Lateritic residuum and silcrete are absent but calcrete is common in the upper metre of erosional soils. Sampling of deeper regolith was hampered by the absence of systematic drilling and paucity of exposures but some was possible at costeans, shafts and at Ian's Mine (*e.g.* Figure 5). Depth to saprolite at these sites is generally shallow (<5 m); data from other parts of the prospect indicates that the base of weathering is variable (10-40 m, average about 30 m) (Circosta and Gum, 1988). The regolith is relatively thin compared with other Au prospects located in the region such as Birthday (Lintern *et al.*, 2000), Challenger (1998), South Hilga (Lintern *et al.*, 2002), Jumbuck (Lintern *et al.*, 2002), and Golf Bore (Lintern *et al.*, 2002). The reason(s) for this are unclear but may be due possibly to the greater relief, absence of a "protective" silcreted duricrust and/or different rock types at Earea Dam.

Regolith in depositional areas is overlain by a fine-grained red-brown alluvium-colluvium, up to three metres thick in the vicinity of the prospect, and thicker still where dune sands have overlain the colluvium, several hundred meters to the south. This colluvium-alluvium is comprised of clays, silts and sands overlying a red-brown hardpan of variable thickness usually located within the top metre of the surface. Carbonate accumulation is weak to moderate in the colluvium and upper part of the hardpan. There is a general absence of lag but coarse, angular bedrock material occur at depth within the colluvium. Depositional regime bordering the hills commonly has a substantial covering of coarse lag of angular bedrock which extends into adjacent creek lines.



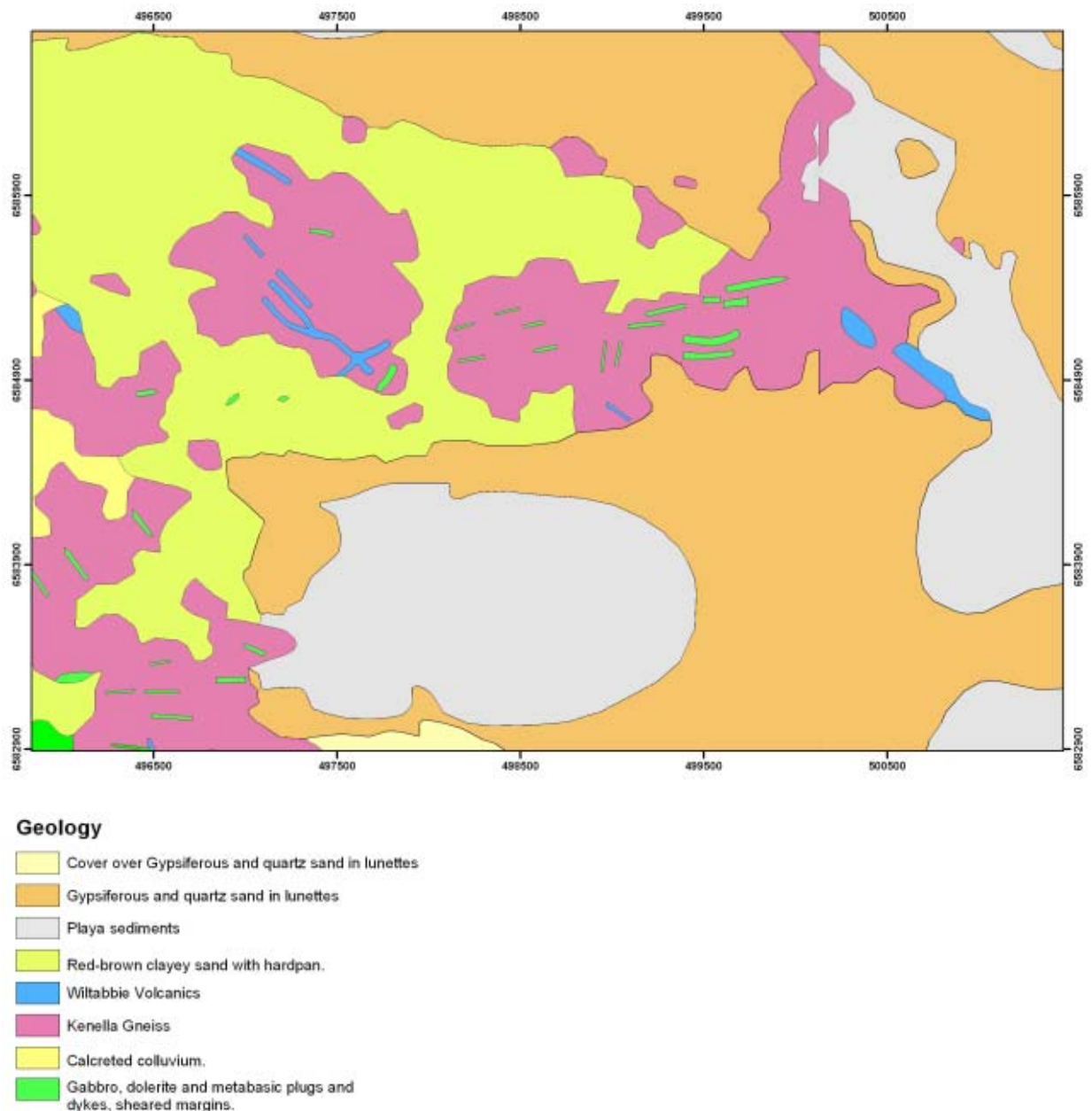


Figure 4: Geology of the Earea Dam Prospect (Source: PIRSA GIS).

### 3.1.2 Basement (*in situ*)

The predominant lithology in the area is Archaean Kenella Gneiss which is part of the Mulgathing Complex (Daly *et al.*, 1979). This bedrock unit commonly crops out in the study area and is easily identifiable on Landsat TM imagery (Figure 5). It is a pinkish-red, quartz-microcline-plagioclase-garnet-biotite gneiss with poor compositional layering and local pegmatitic separations and has a minimum metamorphic age of  $2488 \pm 130$  Ma (Rb-Sr). Mafic granulite bands occur throughout the Kenella Gneiss (Crettenden and Fradd, 1992). These bands consist mainly of mafic minerals with varying amounts of quartz, biotite and pyrrhotite. They are highly metamorphosed, altered, and coarsely re-crystallised. Three sets of dykes intrude the gneiss at Earea Dam: fine to medium dolerite, fine to medium grained amphibolitic dolerite (both of the Kimban orogeny, and porphyritic brown rhyolite and rhyodacite of the Gawler Range Volcanics. The dykes outcrop poorly, vary in width from 2 to 16 m, have near vertical dips, and sheared margins (Crettenden and Fradd, 1992). They cross-cut the layering trend of the Kenella Gneiss (Circosta and Gum, 1988).

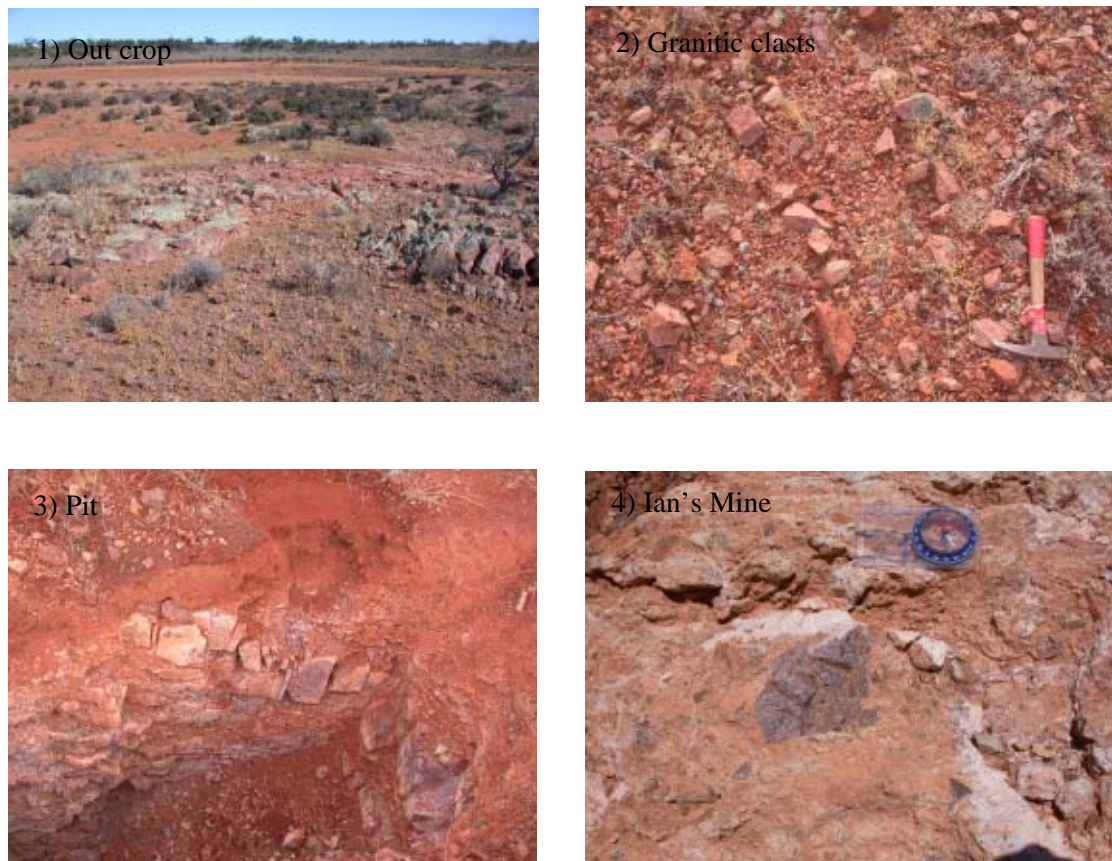


Figure 5: Bedrock occurrences at Earea Dam: 1) outcrop exposure on the edge of a clay pan; 2) lag of angular granitic material; 3) exposure of bedrock in small pit; 4) fresh bedrock within weathered material exposed in pit face at Ian's Mine.

### 3.1.3 *Saprolite*

Saprolite rarely outcrops in the study area, except in the mine workings. Weathering of bedrock has formed two types of product: one is dominated by kaolinite and quartz fragments and derived from felsic rocks such as the Kenella Gneiss, whereas the other is dominated by smectitic clays from the mafic dykes. Saprolite in the pit exposures contain numerous clasts of fresh rock which been commonly coated with carbonate towards the top of the saprolith making the boundary with the pedolith either diffuse or indistinct.

### 3.1.4 *Hardpan*

Red brown hardpan (Eggleton, 2001) is a convenient field term to describe the distinct, red-brown to brown, clay-rich, silicified unit found beneath the soil in the valley. The hardpan is characterised by dark brown to black Fe and Mn oxide and oxy-hydroxide occurring as coatings. The hardpan contains a variety of clasts including quartz, saprolite and bedrock, and is frequently calcareous in its upper part.

At Earea Dam, hardpan is mostly comprised of silicified alluvium-colluvium, confined to the depositional regime and is commonly observed in the costeans close to Ian's Mine (Figure 6). It is covered with variable thicknesses (>20 cm) of loose clay-rich soil. The hardpan is probably ubiquitous in the valley sediments suggested by the difficulty penetrating below about 0.5 m by the power auger. However, any visual evidence of the hardpan will be destroyed by augering.

The petrology of two hardpan samples was undertaken (Appendix 1; Mason, 2002). Sample ED70-1 is creamish brown hardpan composed of small (mostly millimetre-sized, up to ~1 cm) angular pale to dark crystals and lithic fragments in a fine-grained brownish cream calcareous matrix. There is indistinct layering with thin paler bands in the matrix which enwrap larger lithic fragments. Abundant orange brown ferruginous clay materials are fine-grained and form thin rinds around mafic and felsic lithic fragments, but is more abundant as a dense matrix enclosing lithic and crystalline fragments in an indistinct band several centimetres thick. Calcite is abundant, occurring as a very fine-grained porous

cement which mantles polymict fragments (lithic, crystal, and ferruginous silicified clay types). Where more abundant, it tends to form dense turbid cryptocrystalline ball-like concentrations that are mantled by colourless very fine-grained form of calcite.

Hardpan specimen, ED241-1, has a similar framework-supported arenaceous clastic sedimentary texture to ED70-1, with closely-packed crystal and minor lithic fragments firmly cemented in ferruginous clay, but is non-calcareous. Both mafic and felsic lithic fragments are common, some up to 3 mm across. However, much of the hardpan is composed of very fine-grained orange-yellow ferruginous clay which tend to form discontinuous thinly layered fillings between the crystal and lithic fragments. Commonly, the laminated clay fillings progress into void spaces which represent unfilled remnant interparticle pores (Mason, 2002).

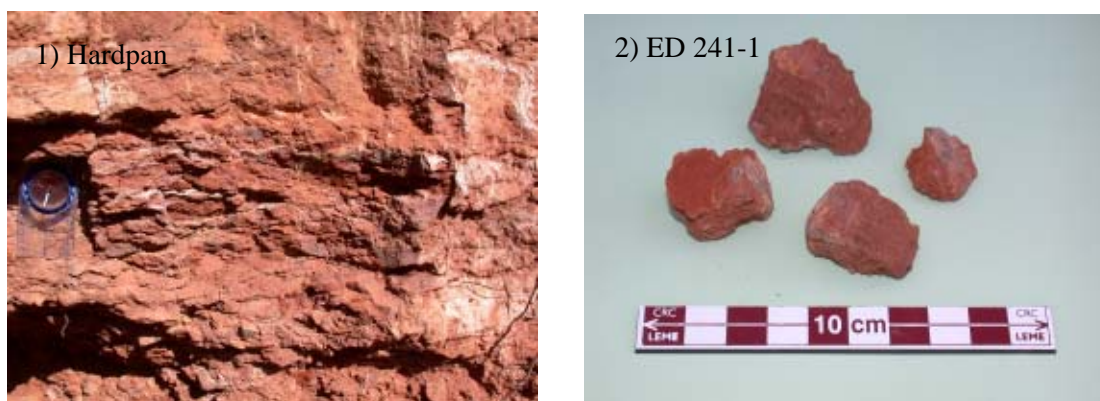


Figure 6: 1) hardpan exposed in costean (see also photo 6 in Figure 8 to see context); 2) hardpan material showing dark purple Mn coatings.

### 3.1.5 Dune sand

Aeolian dunes blanket the southern part of the geochemical study area and conceal older depositional and residual regolith regimes (Figure 7). Exposures on the edge of nearby salt lakes and clay pans indicate the dunes can be >5 m thick in places. Wind-blown sand is also a significant component of the soils throughout the entire prospect and is presumably derived from the nearby dunes and, ultimately, the eroding gneissic terrain. The dunes are easily mapped from the Landsat imagery. The sand is generally loose, free running, and is partly stabilised from erosion by deep-rooted vegetation. The dunes are considered a recent addition to the landscape and their occurrence and extent is significant since they are likely to dilute any geochemical signals in the older regolith units.



Figure 7: Dune sands at Earea Dam: 1) southerly view from hill located to east of Ian's Mine with playa (distance) bordered by vegetated sand dunes (arrowed); 2) gypseous sand dune bordering playa.



### **3.1.6 Calcrete**

Calcrete occurs in a variety of forms at Earea Dam including powdery (loose and coatings), nodular, laminar and cobbles (massive) (Figure 8). Where saprock or competent saprolite is located close to the surface, calcrete partly or wholly coats the *in situ* material to form cobbles and boulders. Thus, calcrete in these areas often includes large clasts (to 10 cm) of saprolite that may drastically elevate the geochemical concentrations of certain elements, including Au. In Ian's Mine, calcrete encloses the hematitic host material with some analyses reporting several hundred ppb Au. In addition, calcrete occurs in nodular, laminar and massive forms in the thin transported material in Ian's Mine. Further downslope, in the depositional regime, the calcrete is much less abundant and occurs as powdery forms coating soil particles and partings on the upper parts of the hardpan. The dune sand to the south of the prospect is slightly calcareous indicating that at least some of the carbonate is of aeolian origin.

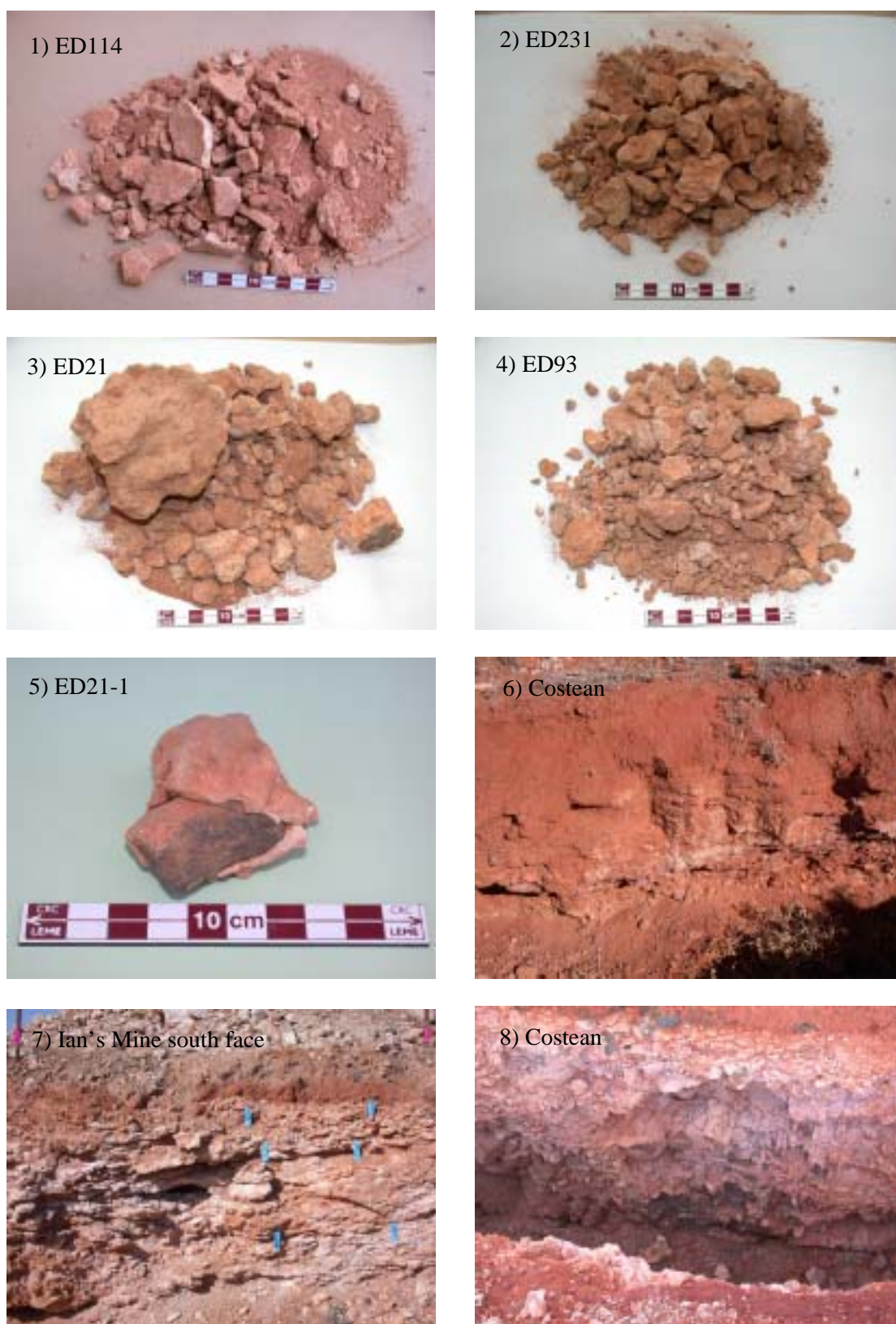


Figure 8: Samples and field occurrence of calcrete: 1) sample ED114; 2) sample ED231; 3) sample ED21; 4) sample ED93; 5) sample ED21-1, comprised of granulite clast partly encased by calcrete; 6) costean partly located in depositional terrain showing calcrete on partings of hardpan; 7) laminar and massive calcrete in pit face of Ian's Mine; 8) costean showing calcrete coatings on mafic dyke saprock.

### 3.1.7 Soils

Soils are variably textured in the area. Poorly-structured sandy soils dominate the dune system to the south. A thin (<5 cm) sand-rich clay covers the valley sediments above a very compacted red-brown clay-rich sub-soil. This in turn overlies a hardpan. Thin clay-rich and calcareous lithosols blanket the saprolite on the flanks of the valley and the hills area. The SWIR spectra indicate the presence of poorly-ordered kaolinite and possibly illite.

## 3.2 Regolith-landforms

### 3.2.1 Introduction and methods

A regolith-landform map was constructed for a ~6 km by 4 km area about the Earea Dam Prospect (Figure 9). The map was constructed using a combination of field observations, Landsat TM, aerial photography and ASTER (Advanced Spaceborne Thermal Emission and Reflection Radiometer) imagery (Figure 10). Several regolith-landform units were identified from the remote sensing imagery (Figure 9). The RTMAP scheme was used for regolith-landform mapping whereby regolith-landform units are coded using letters. The first letter(s) (in capitals) refers to the regolith and the second letter(s), (in lower case), the landforms e.g., Lpp refers to lacustrine sediments in a playa landform (Pain *et al.*, 2000).

Remotely sensed images were warped in ArcGIS™ to fit GPS-calibrated ground control points with estimated easting-northing error of <6 m. ASTER Level 1B data were used to investigate the occurrence of mineral groups containing AlOH, MgOH, carbonates and silicates for mapping purposes (Hewson *et al.*, 2003), with correction for miscalibration effects using Earth Remote Sensing Data Applications Centre's (ERSDAC) Crosstalk Correction software (Hewson *et al.*, 2003). ASTER data were also used to produce the digital elevation model (DEM), from which the major landforms can be discerned. The band ratios used here for Landsat TM and ASTER data are a relatively simple image processing method to emphasise spectral differences associated with different regolith/mineral groups measured by different bands.

Most of the information for map construction was obtained using aerial photography, observation points and Landsat TM (Tapley and Gozzard, 1992). Landsat TM band ratios 5/7, 4/7 and 4/2 as RGB have been previously used to construct regolith-landform maps in the Pilbara (Tapley and Gozzard, 1992) and Mt Weld areas (pers. comm., T. Munday, CSIRO). These ratios are useful at Earea Dam for showing the main regolith-landform units of erosional hills, sand dunes, playas and clay-rich areas. The colours broadly correlate with materials on the ground with blue related to quartzose dune sand, red to clay-rich areas, yellow to clay-rich playas and yellow-orange to clay-rich felsic saprolite of the erosional hills. The location of the sand dunes and lunettes are particular important from the geochemical sampling perspective.

ASTER is a Japanese imaging instrument on board the NASA Terra satellite platform, launched in December 1999 as part of NASA's Earth Observing System (EOS). The ASTER DEM was constructed using band 3 from a pair of Level 1A images generated from the nadir- and backward-looking sensors. Some information similar to the Landsat TM bands ratios 5/7, 4/7 and 4/2 was produced using ASTER bands ratios 5/6, 3/6 and 3/1 but was not as useful at discerning regolith materials. ASTER bands 3, 2 and 1 were modified with the decorrelation stretching option to discern quartz-rich (red hues) and clay-rich (blue hues) areas. ASTER bands 1, 2 and 3 had the added advantage of a superior 15 m pixel size compared with Landsat at 30 m.

### 3.2.2 Regolith-landforms

Mapping of the regolith at Earea Dam identified eight regolith-landform units at the 1:25000 scale (Table 1). These include saprolith outcrop, colluvial slopes to the saprolith, playa lakes and aeolian dunes. The proportion of each unit is shown in Table 2 and indicates that low hills of saprolith and associated slopes are the spatially largest units represented at Earea Dam. The “mosaic” relationship of the colluvial slope unit (Cer) and the saprolith unit (Sel) suggests that the depth of cover for the mapped area due to colluvium and alluvium depositional processes is probably not significant i.e. < 10 m.

Significant dune thicknesses (>8 m) have formed at the western margins of the eastern-most playa, where breakaways have formed in lunettes from the playa located to the west (Figure 7). Aeolian sediments (sand dunes and gypsum dominated lunettes) form a combined significant group of regolith-landform units comprising nearly 25% of the total area investigated. The thickness of aeolian sediments is not known but the greatest accumulations occur on the margins of playas, particularly to the east of the main playa where lunettes have formed. Some of these lunettes are relict landforms originally created when the playa was located further to the east. The shape of the lunettes indicates that the wind direction is predominantly from the west.

Table 1: Regolith-landform code, regolith type and description of units at Earea Dam Gold Prospect.

Code	Type	Description
Aed	Wide creek beds and depressions	Flat or very gently sloping alluvial unit receiving sediments and run-off from adjacent ground. Wide ephemeral creek beds and small depressions. No vegetation or low open shrubland.
Cer	Colluvial slopes	Gently sloping unit of colluvium dominating slopes bordering saprolite-dominated units. Comprised of variable thickness (>1 m) of sediment of mixed grain size and origin. Some aeolian material may be present. Low shrubland.
Cpp	Margins of playa lakes	Flat or gently sloping colluvial unit bordering playas with low open shrubland.
ISud <sub>1</sub>	Sand dunes	Flat or gently sloping landform pattern comprised of sandy material of aeolian origin. Where sand supply has been significant, it has formed into linear dunes. Where supply has been smaller, unit forms sand spreads intermixed with colluvial units. Open low woodland.
ISud <sub>2</sub>	Sand-gypsum dunes	Flat or gently sloping unit comprised of variably sand- and gypsum-dominated material of aeolian origin. Borders lunettes and playa margins. Open low woodland to open low shrubland.
ISuu	Gypsum dunes	Flat or gently sloping unit comprised of surficial to sub-surface gypseous sand and clays of aeolian origin. Predominantly relict lunette landform. Playas have migrated westwards to leave landform isolated. Open low woodland to open low shrubland.
Lpp	Playa lakes	Flat unit comprised of saline and non-saline fine and coarse sediments of variable thickness. Small areas of outcrop indicate sediment thickness maybe <1 m in places. Unvegetated.
Sel	Bedrock-saprock-saprolite on low hills	Gently to moderately sloping landform pattern of low relief (30-40 m). Outcrop and subcrop of Kenella Gneiss and mafic intrusives. Surface commonly littered with coarse lag. Soils are skeletal. Fixed erosional stream channels, closely to very widely spaced, which form a dendritic or convergent integrated tributary pattern. There is continuously active sheet flow, creep, and/or channelled stream flow during rare rainfall events. Low shrubland with minor trees.

Table 2: Regolith landform unit, RTMAP code, number of occurrences (count), total area and % occurrence for the Earea Dam Gold Prospect. Units are ranked in order of % occurrence.

Regolith-landform unit	RTMAP code	Count		
		t	Area (m)	%
Sand-gypsum dune	ISud2	2	335458	1.5
Wide creek bed and depression	Aed	10	447819	2.0
Margins of playa lake	Cpp	7	1265096	5.6
Gypsum-dominated dune	ISuu	9	1647628	7.3
Sand-dominated dune	ISud1	12	3393713	15.0
Playa lake	Lpp	4	3800025	16.8
Colluvial slopes	Cer	7	5340581	23.6
Bedrock-saprock-saprolite outcrop on low hills	Sel	16	6366065	28.2

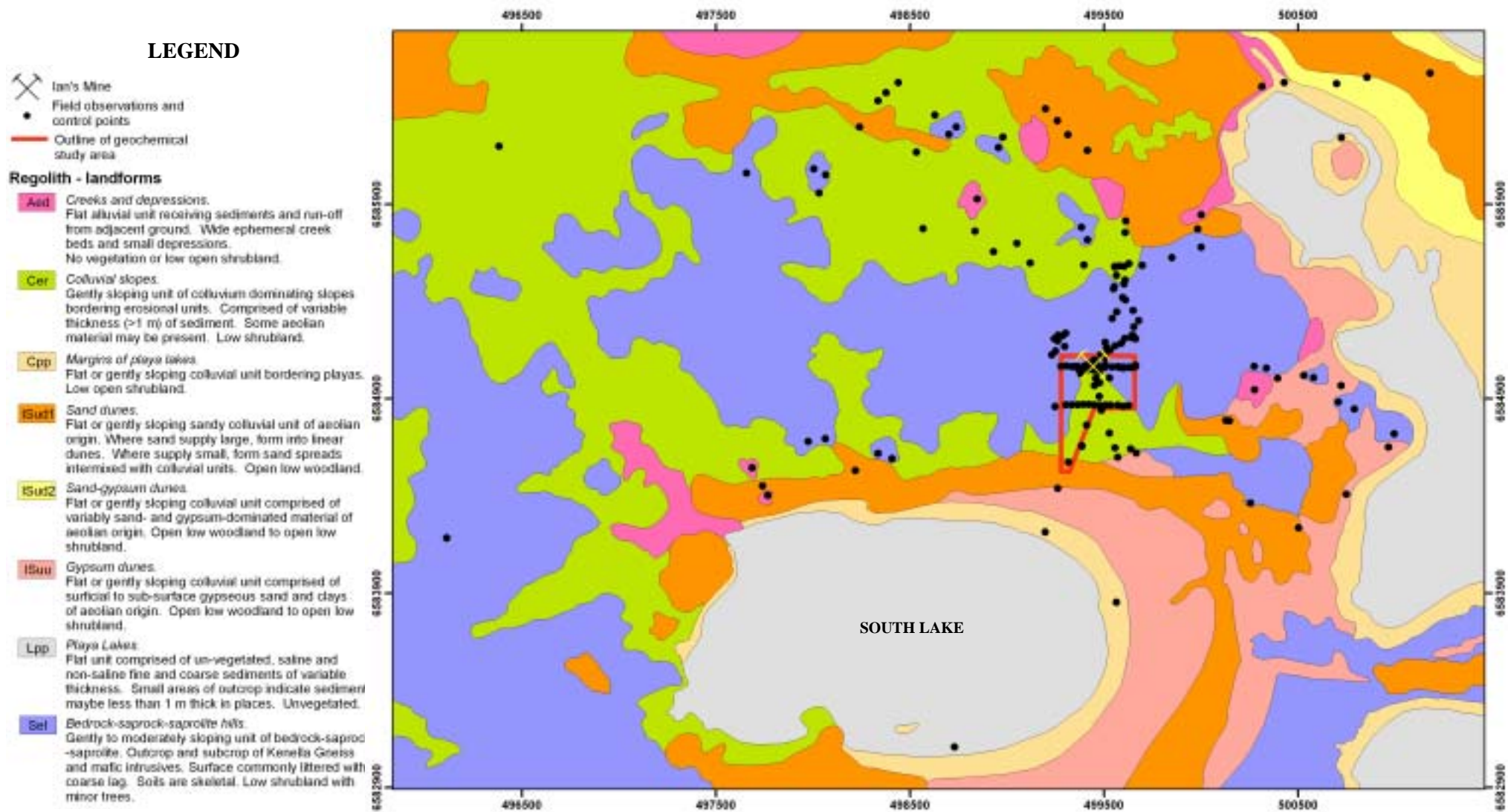


Figure 9: Regolith-landform map of the Earea Dam Prospect showing location of observation points (open circles), Ian's Mine and geochemical study area. The regolith map forms part of the GIS (Appendix data disc). For full regolith-landform description see text.



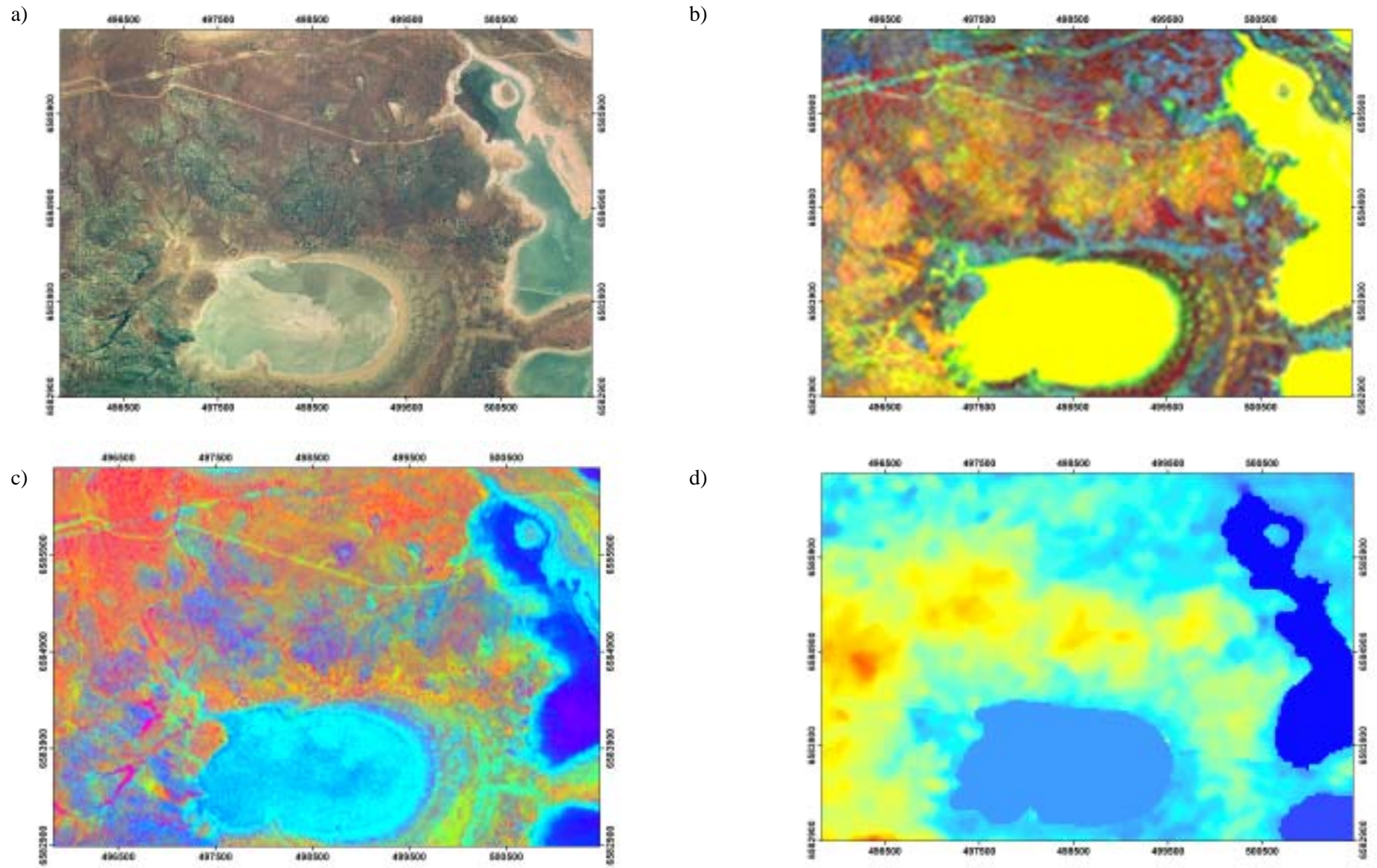


Figure 10: a) aerial photography, b) Landsat TM composite ratio image (bands 5/7, 4/7 and 4/2), c) ASTER bands 3, 2 and 1 (decorrelated stretch) and d) DEM (generated from ASTER Level 1A images) used in the construction of the regolith-landform map (Figure 9)

## 4 GEOCHEMISTRY

### 4.1 Introduction

The geochemical data is described for each face of Ian's Mine in sections 4.4 to 4.6 that follow. More photographs of sampling sites, particularly for the south face, are on the Appendix data disc. The geochemistry of the soils is described element by element in section 4.7. The final section (4.8) describes the geochemistry of a size fraction study of selected samples.

### 4.2 Mineralogy

Selected samples from four profiles from Ian's Mine (Figure 11) were chosen for XRD analysis (Table 3); geochemical analysis of the same samples is reported in Sections 4.4 to 4.6. The mineralogy indicates that the regolith is mostly dominated by quartz, calcite, kaolinite, plagioclase, alkali feldspars and micas, consistent with the gneiss lithology and secondary calcrete accumulations observed in the field. Gypsum forms a metre thick horizon in the southeast corner of the pit but its origin is unclear. The presence of bassanite appears to be a heating artefact generated during the milling of gypsiferous materials. Hematite is locally abundant and is, in part, associated with mineralization. A mafic dyke intrudes into the base of the pit (and at the base of profile - samples ED01-ED11) and is dominated by hornblende and plagioclase which has weathered to produce goethite, kaolinite and smectite.

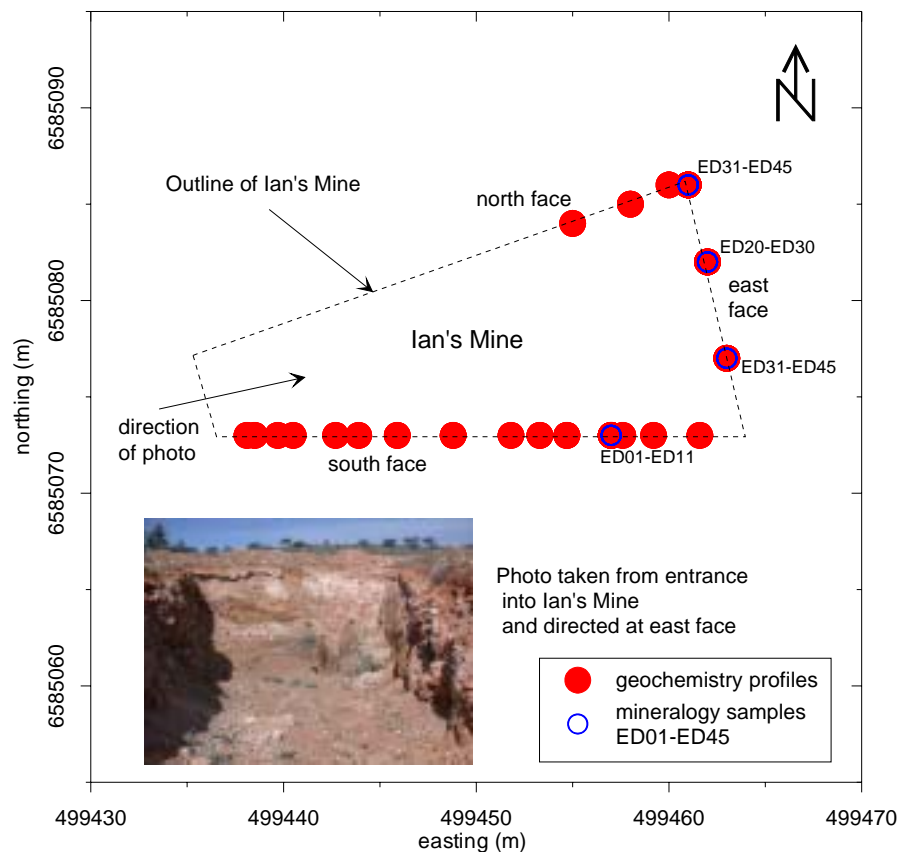






Figure 11: Location plan of profiles sampled at Ian's Mine. The east face is about 4 m deep.

Table 3: Selected mineralogy of 4 profiles from Ian's Mine, Earea Dam. Estimates of mineral abundances were based on peak height:  abundant;  moderately abundant;  some;  trace. See Figure 11 for location of samples, Figure 15 for geochemistry and location (Profile D) of samples ED01 to ED11, Figure 16 for geochemistry and location of samples ED12-30 and Figure 17 for geochemistry and location of samples ED31-45.

Sample	depth (cm)	Regolith unit	QUARTZ	CALCITE	ALBITE ordered	ALBITE disordered	MICROCLINE	MAGNESIO HORNBLende, FERROAN	BIOTITE	BASSANITE GYPSUM	HEMATITE	GOETHITE	KAOLINITE	ILLITE	OTHER
ED01	10	colluvium						XXXXXXXXXX							
ED02	25	saprolite													
ED03	60	saprolite													
ED04	105	saprolite													
ED05	165	saprolite													
ED06	210	saprolite		XXXXXX											
ED07	235	saprolite													
ED08	280	saprolite									XXXXXX				
ED09	300	saprolite	XXXXXX					XXXXXXXXXX					XXXXXX		smectite
ED10	325	saprock											XXXXXX		
ED11	465	saprock													
ED12	10	colluvium													
ED13	30	colluvium											XXXXXX		
ED14	50	colluvium											XXXXXX		
ED15	95	saprolite													
ED16	170	saprolite		XXXXXX		XXXXXX			XXXXX				XXXXXX		
ED17	230	saprolite				XXXXXX							XXXXXX		
ED18	250	saprock													
ED19	370	saprock				XXXXXX									
ED20	10	colluvium											XXXXXX		
ED21	30	colluvium											XXXXXX		
ED22	50	colluvium					XXXXXXXXXX						XXXXXX		
ED23	70	colluvium											XXXXXX		
ED24	90	saprolite		XXXXXX		XXXXXX							XXXXXX		
ED25	115	saprolite				XXXXXX				XXXXXX					
ED26	180	saprolite				XXXXXX									
ED27	230	saprolite							XXXXX						orthoclase
ED28	245	saprolite					XXXXXXXXXX		XXXXX		XXXXXX		XXXXXX		orthoclase
ED29	260	saprolite					XXXXXXXXXX		XXXXX		XXXXXX		XXXXXX		orthoclase
ED30	290	saprolite													orthoclase
ED31	5	colluvium		XXXXXX											orthoclase
ED32	11	colluvium													
ED33	15	colluvium				XXXXXX	XXXXXXXXXX								
ED34	30	colluvium				XXXXXX	XXXXXXXXXX						XXXXXX		
ED35	50	saprolite											XXXXXX		
ED36	70	saprolite											XXXXXX		
ED37	90	saprolite		XXXXXX							XXXXXX		XXXXXX		
ED38	125	saprolite		XXXXXX							XXXXXX				
ED39	160	saprolite									XXXXXX				muscovite
ED40	160	saprolite					XXXXXXXXXX								muscovite
ED41	175	saprolite									XXXXXX				muscovite
ED42	195	saprolite					XXXXXXXXXX								muscovite
ED43	235	saprolite													muscovite
ED44	270	saprolite													muscovite
ED45	300	saprolite													muscovite

### 4.3 Mineralization

Mineralization is associated with dark hematitic quartz rich material occurring as narrow veins in the Kenella Gneiss. The veins dip to the east and may have formed a tabular structure through the pit which has subsequently been mined out. The mineralization was intersected in several profiles in Ian's Mine. Grab samples from Ian's Mine were analysed for Au and other elements in order to determine any associations of elements and to examine the nature of occurrence of the Au further (Figure 12). The three grab samples with the highest Au concentration were ED95, ED41 and ED71 (30, 32 and 33 ppm Au, respectively). High Au concentrations are usually correlated with high concentrations of Ag, Bi, Cu, Sn, Te, U and W (Figure 12) and is consistent with earlier studies previously discussed (*e.g.* Cretenden and Fradd, 1992). Sample ED95 was sectioned, polished and examined under the SEM in order to identify the nature of the Au and its associated elements (see petrological description in Appendix 1). Some Au with low Ag contents (<1%) was found in hematite (possibly after sulphides) (Figure 13).



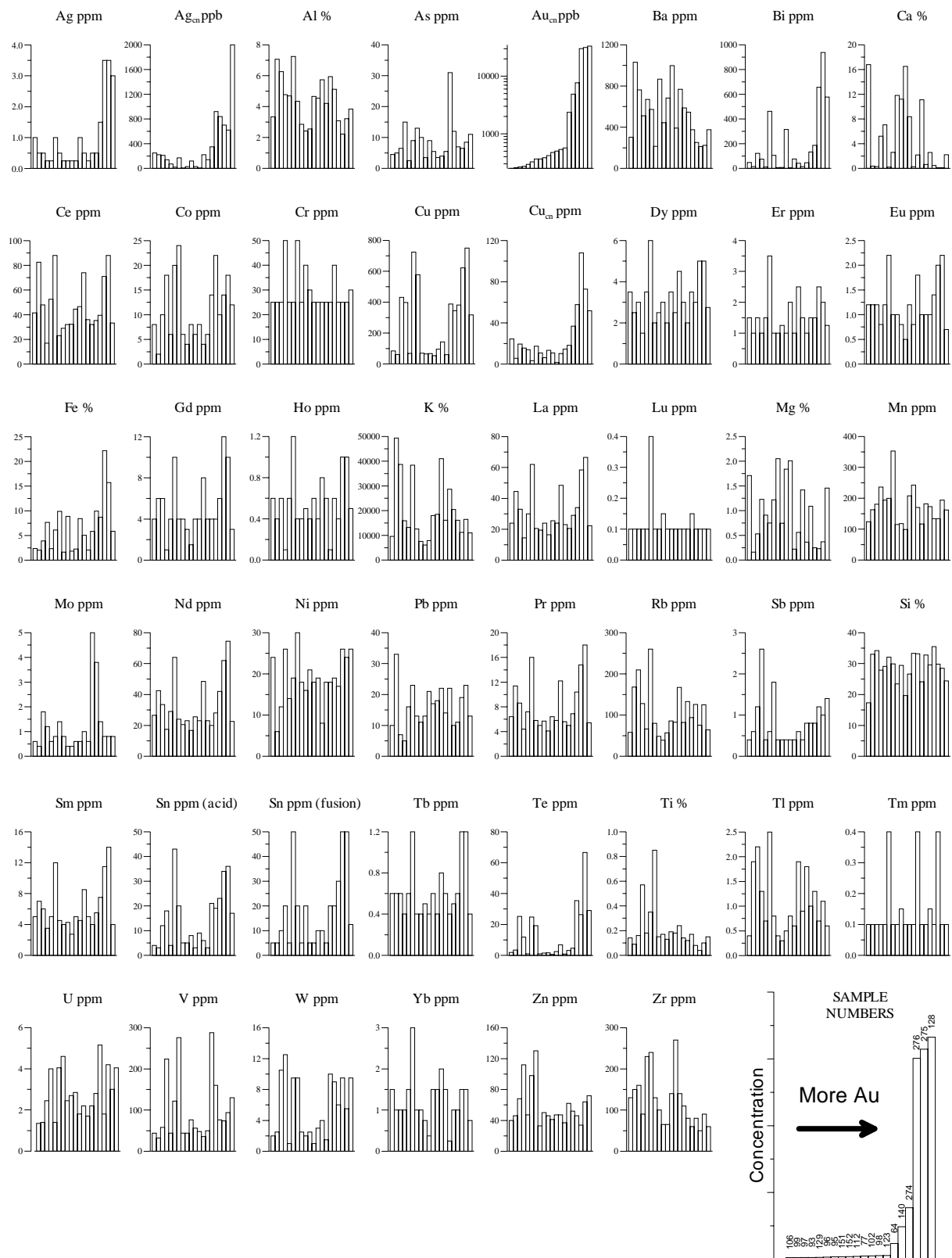


Figure 12: Bar charts showing concentration of selected elements in grab samples from Ian's Mine at Earea Dam Prospect. Samples are ranked (left to right) according to increasing Au content. Cadmium data are below 0.5 ppb. Sample numbers are indicated on the larger histogram.

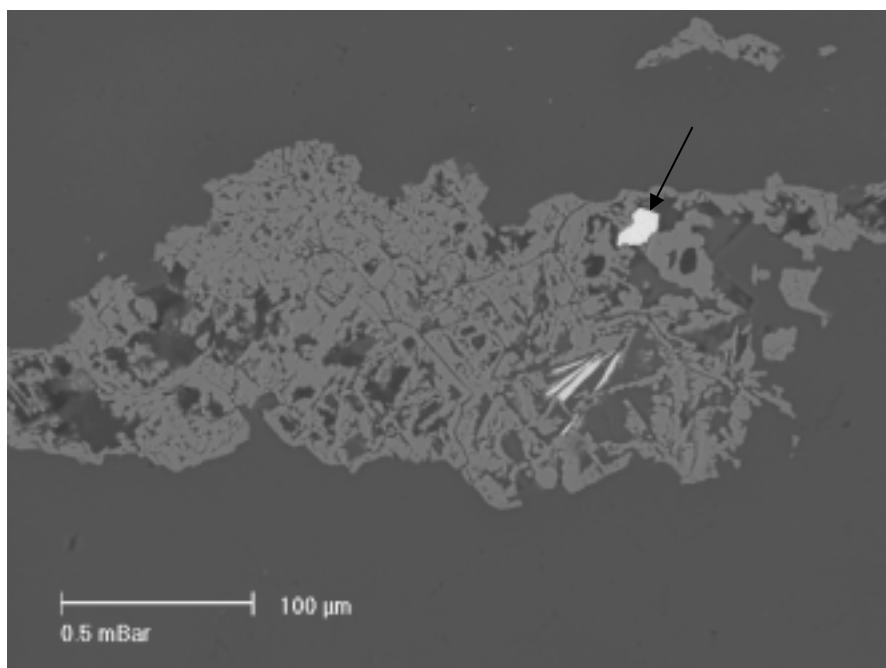


Figure 13: SEM photomicrograph of hematite within quartz containing a 20-30  $\mu\text{m}$  Au grain (arrowed, and with <1% Ag) and “shards” of a Bi oxide. Other Bi minerals found contained Ba and/or V.

#### 4.4 South wall of pit

Fifteen regolith profiles (59 samples) from variable depth were sampled across the south face of Ian’s Mine (Figure 14) and the geochemical data generated contoured in Figure 15. Tabulated data is located in Appendix 2. Elements can be grouped together and related to specific regolith units: felsic saprolite, mafic dyke, smectitic clays, and calcified colluvium and clay saprolite (Table 4).

Gold concentrations are highest (Profile K, Figure 15, 33 ppm) in samples containing hematite-quartz clasts that occur at the contact between the smectite clays and felsic clay saprolite, and part of the veining and tabular body mentioned earlier. These angular clasts also occur within calcrete in the eastern part of the profile within transported material (probably where the mineralization breaches the interface) and suggest that mechanical (gravitational) dispersal of Au (and associated elements) is taking place down slope of the workings. Elements associated with Au include Ag, Bi, Cu, Sn, Te and W with maxima of 2, 578, 388, 21, 29 and 10 ppm, respectively.

The high concentrations of Au in hematite-quartz clasts provide an opportunity to examine the effects of other dispersion processes in adjacent surrounding material. High Au concentrations occurring in the clasts are not correlated to Au concentrations in adjacent materials including overlying calcrete, suggesting that hydromorphic processes such as capillarity or diffusion are not playing a significant role in the dispersion of Au. For example, above Au-rich sample ED71 (33 ppm Au, base of Profile K), Au concentrations are only a weakly anomalous 38, 31 and 50 ppb Au, and this includes calcrete samples. Similarly in profile D where Au concentrations reach a maximum of 2.4 ppm (ED8), other samples (including calcrete) in the profile average <50 ppb. If hydromorphic processes were active, higher Au concentrations would have been expected.

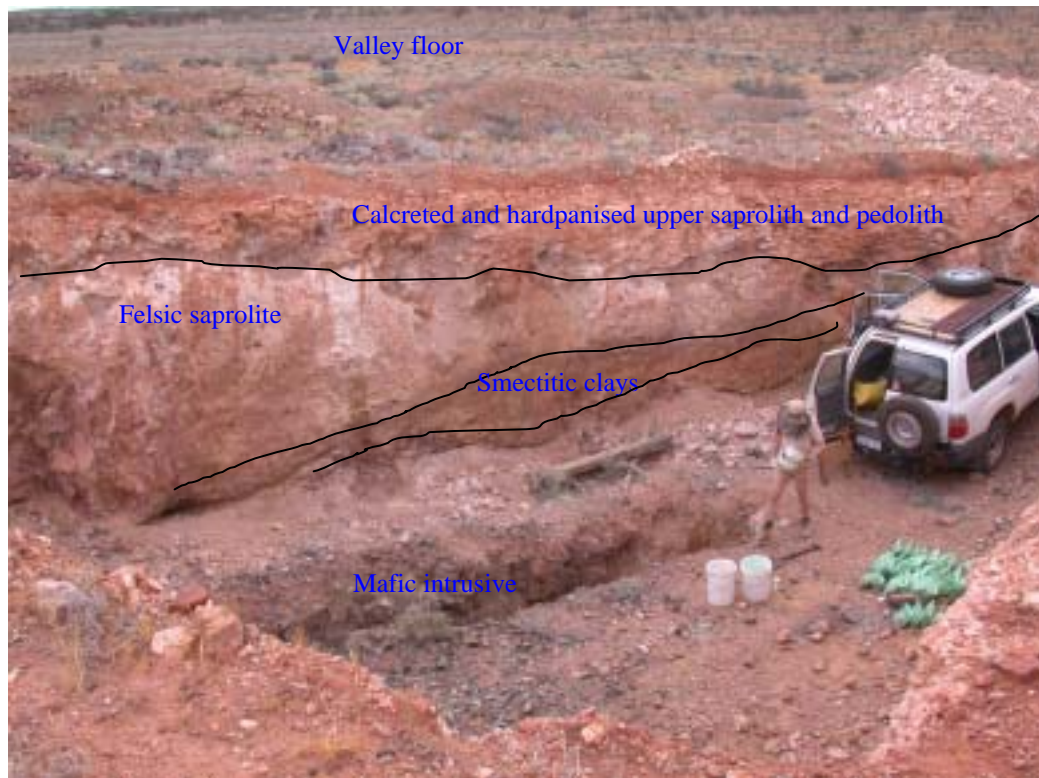


Figure 14: View of south face (Ian's Mine) in foreground with valley and dunes in background. Fifteen profiles were sampled from the south face and the geochemical data are contoured in Figure 15. The vehicle is parked in the western part of the pit facing the access ramp.

Table 4: Summary of elemental association and interpretation in south face of Ian's Mine.

Regolith unit	Associated elements	Comments
Pale felsic saprolite and gypsum	Ca, Al and Si.	Calcium present mainly in gypsum which dominates the eastern part of the face; Al and Si in kaolinite. There are also moderate amounts of Fe and K. Gravels of near fresh gneiss present.
Dark grey mafic intrusive	Fe, Mg, Al, Cu and Ti	Only one sample taken
Green-khaki smectite clays	Ag, Au, Bi, Cu, Fe, Sn, Te, and W	Gold and elements associated with hematite-quartz clasts at the contact between mafic-derived smectite clay and felsic saprolite
Pinky white calcrete	Ca, Ag, Au, Al, Bi, Cu, K, Mg, Si, Sn, Te, Ti, W, Zr.	Gold and elements associated with mineralization appear to be most concentrated in the western end of the pit face where hematite-quartz clasts are present within calcreted colluvium.

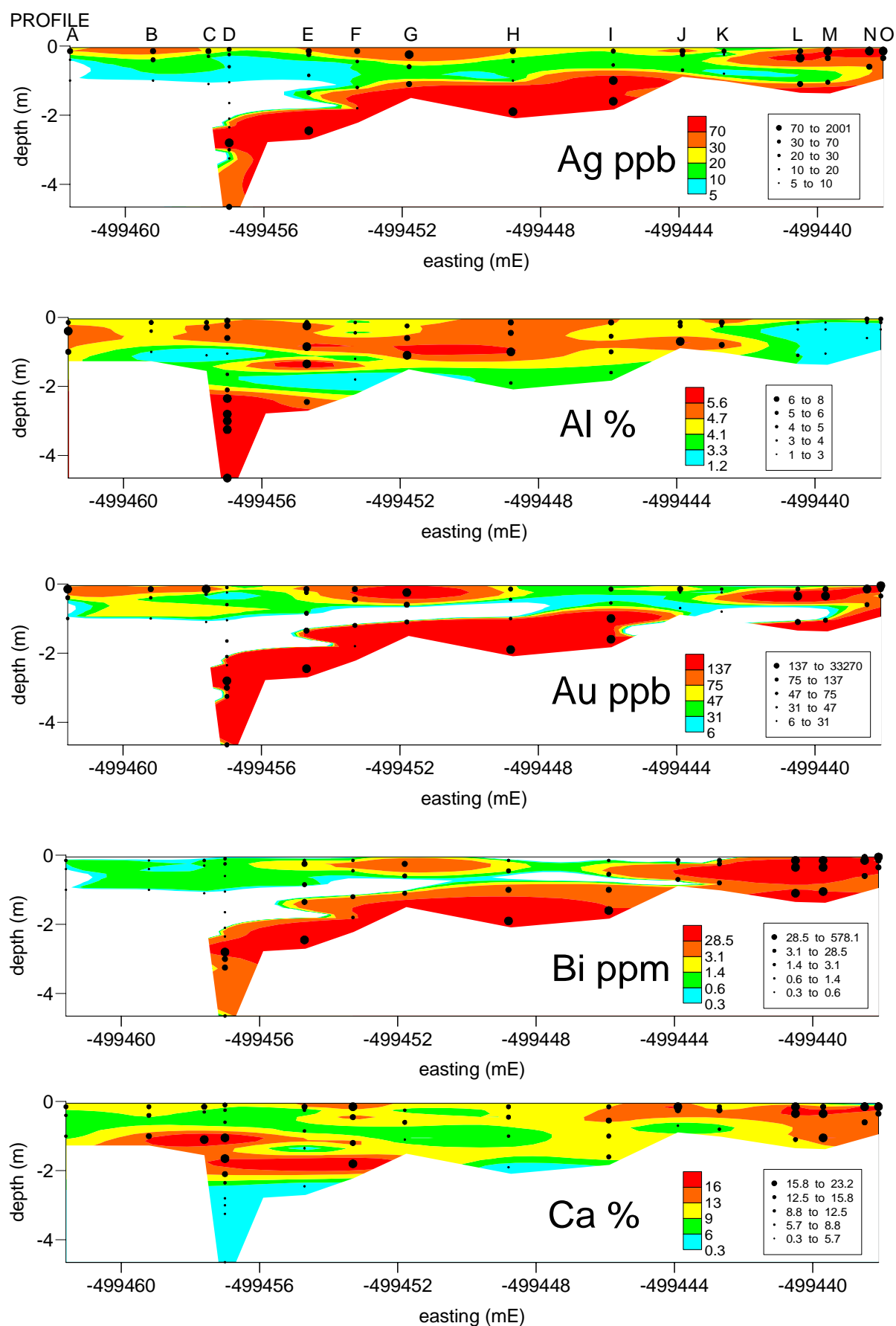


Figure 15: Distribution of selected elements in the southern pit wall of Ian's Mine.

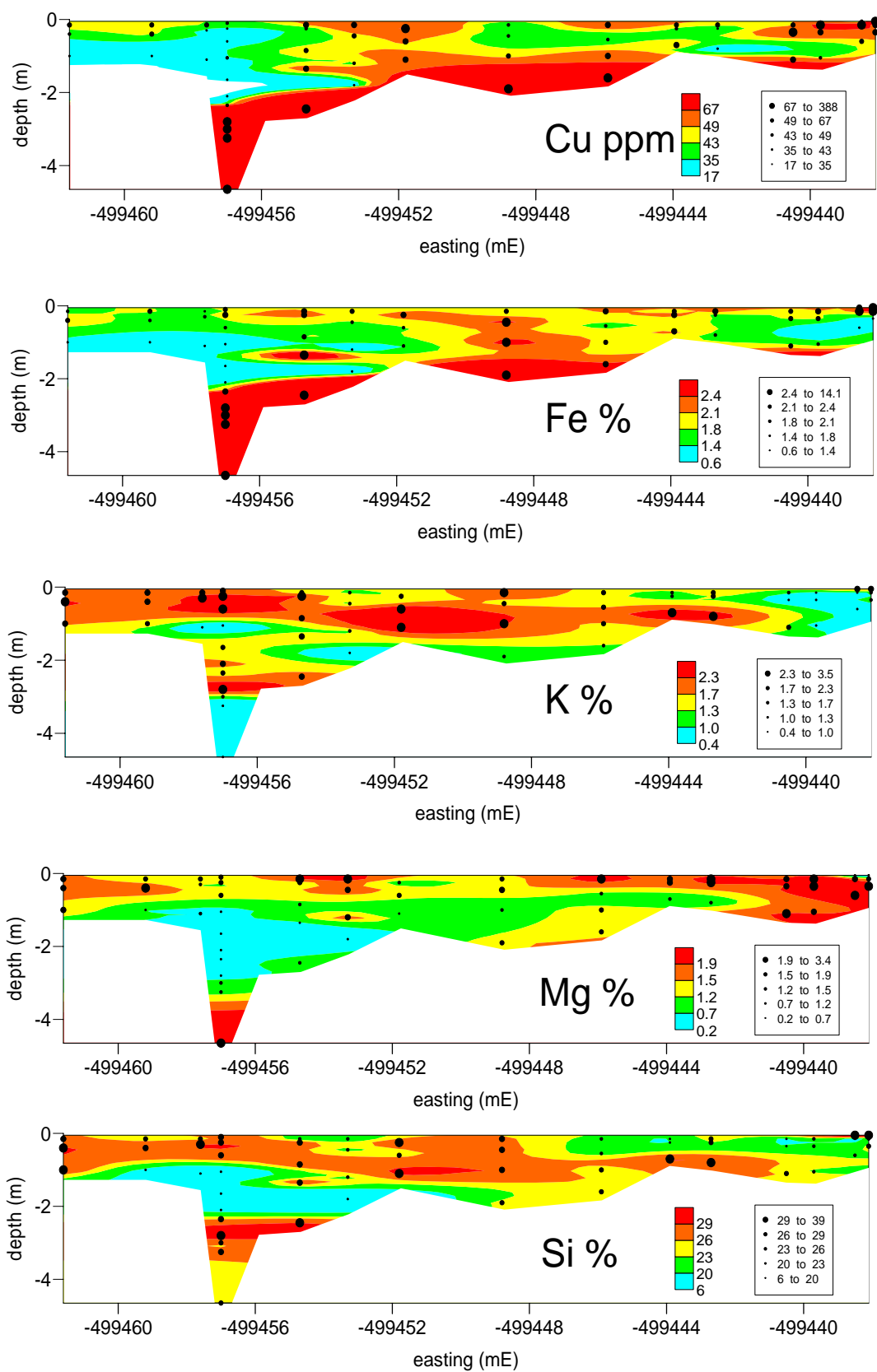


Figure 15 (continued): Distribution of selected elements in the southern pit wall of Ian's Mine.

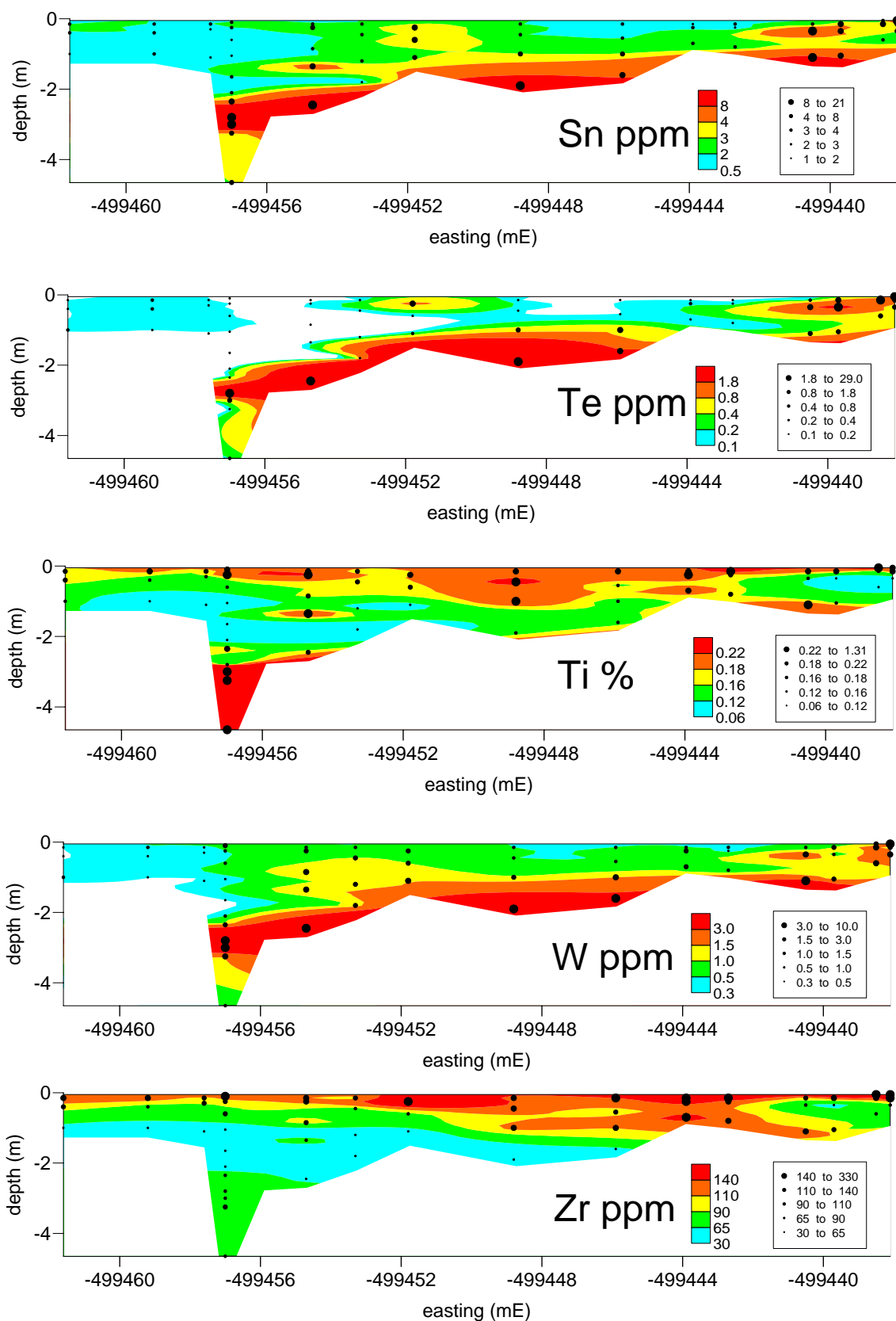


Figure 15 (continued): Distribution of selected elements in the southern pit wall of Ian's Mine.

#### **4.5 Eastern wall of pit geochemistry**

Two regolith profiles were sampled from the eastern pit face and the geochemical data and location displayed by element in Figure 16. Tabulated data is located in Appendix 2. The regolith is similar to the southern face of the pit except the mafic dyke is absent. Near surface calcrete tops the eastern wall and is underlain by friable clay saprolite. Gypsum, present in the eastern part of the southern wall, continues around the SE corner of the pit in samples ED15 to ED17 (Figure 16). The depth of weathering is much shallower in the NE corner and there are also higher K concentrations. The saprolite and gypsum zones contain cobbles of almost fresh gneiss.

Gold and Ag, Bi, Cu, Sn, Te and W are anomalous in a narrow clay- and Fe-rich band within the saprolith unit in NE corner of the pit. This band was probably part of a tabular structure (since mined) containing hematite-quartz gravels dipping through the pit. Peak concentrations in the band for Au, Ag, Bi, Cu, Sn, Te and W are 0.1 ppm, 130 ppb, 900 ppb, 10 ppm, 0.6 ppm and 10 ppm respectively. The highest Au concentration (475 ppb) from these two profiles occurs in one calcrete sample. Concentrations in adjacent material are lower (71 and 33 ppb) possibly suggesting that the Au is located in a rock fragment derived from upslope.

#### **4.6 Northern wall of pit geochemistry**

The northern pit face consists of clay saprolite overlain by silicified clay saprolite and then calcareous hardpanized colluvium-alluvium. The clay-rich saprolite contains cobbles and gravels of near-fresh gneiss. Several grab samples and one profile were sampled. Two regolith profiles were sampled from the eastern pit face and the geochemical data and location displayed by element in Figure 17. Tabulated data is located in Appendix 2. The profile intersected the mineralized band where peak Au concentrations reached 31 ppm with elevated Ag (620 ppb), Bi (938 ppm), Cu (750 ppm), Sn (36 ppm), Te (67 ppm) and W (11 ppm). Other grab samples rich in Au also showed elevated concentrations of these elements. Gold concentrations in calcrete immediately above the mineralised band reach a maximum of 272 ppb but other calcrete samples have Au concentrations well below this value. The erratic nature of the Au distribution again (as with other profiles) suggests the presence of detrital Au particles or Au present within rock fragments. Gold concentrations in soil (0-10 cm) above the Au rich material reach 15 ppb.



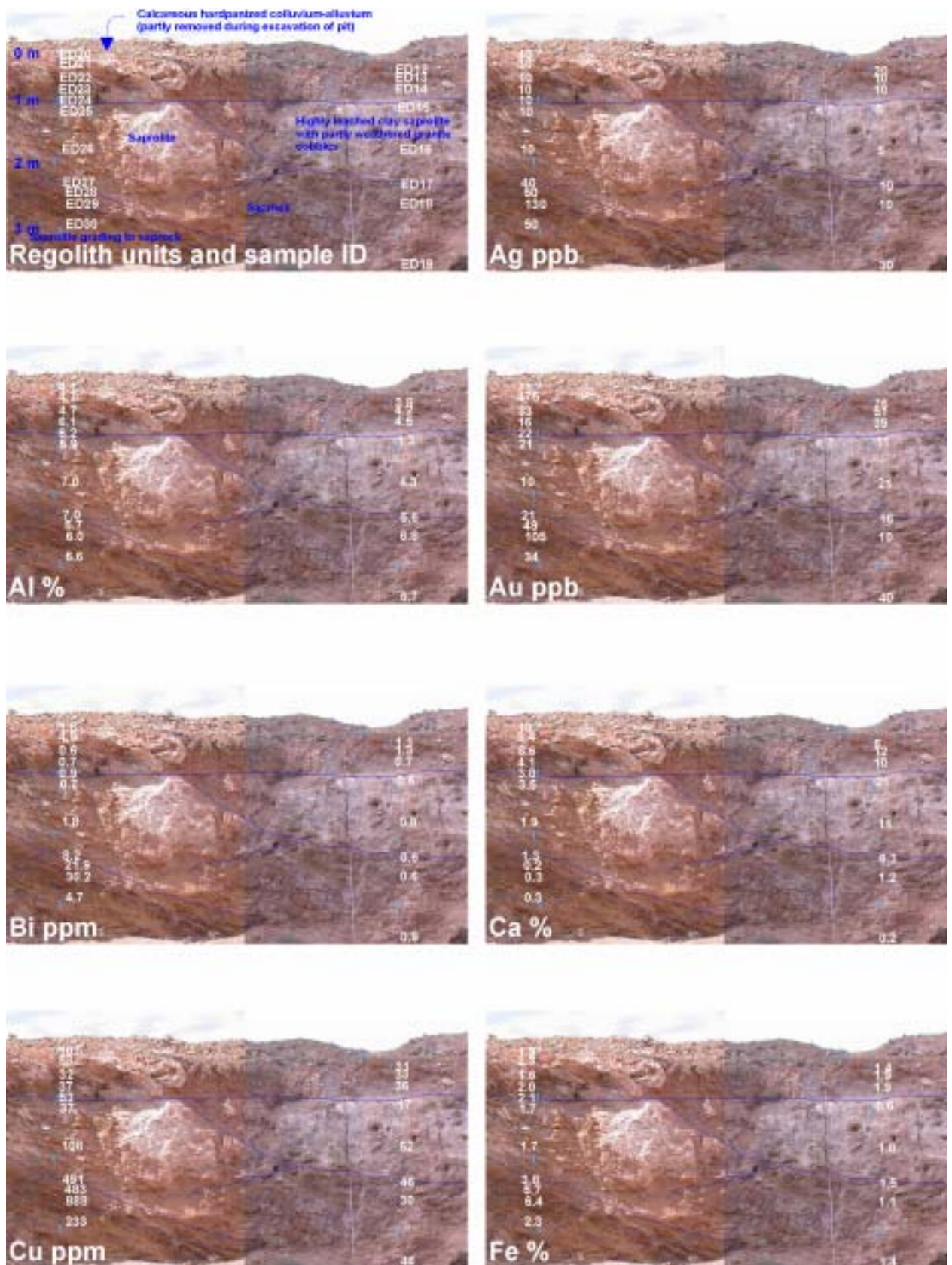


Figure 16: Sample ID and distribution of selected elements in the eastern pit wall of Ian's Mine.



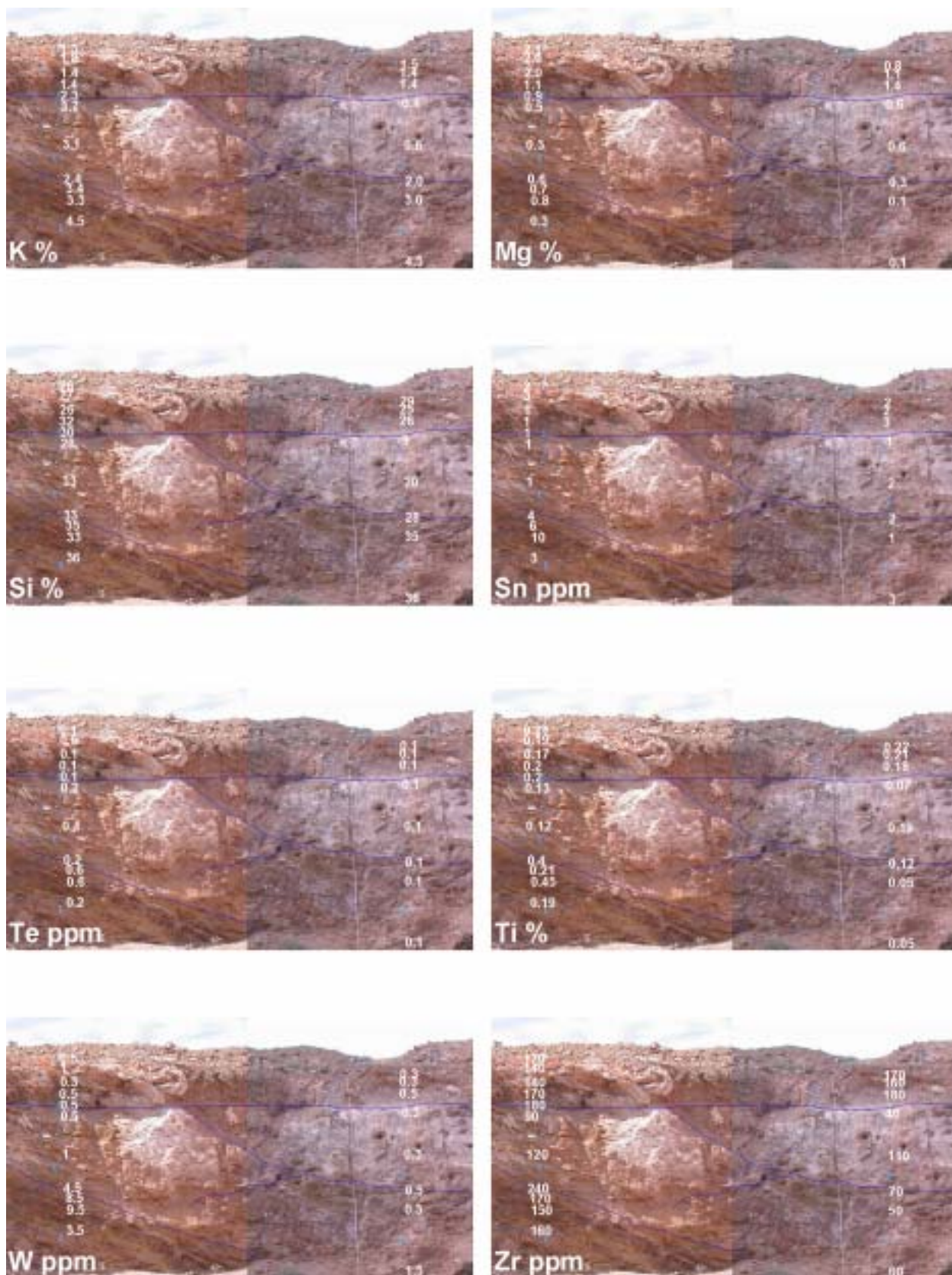


Figure 16 (continued): Sample ID and the distribution of selected elements in the eastern pit wall of Ian's Mine.



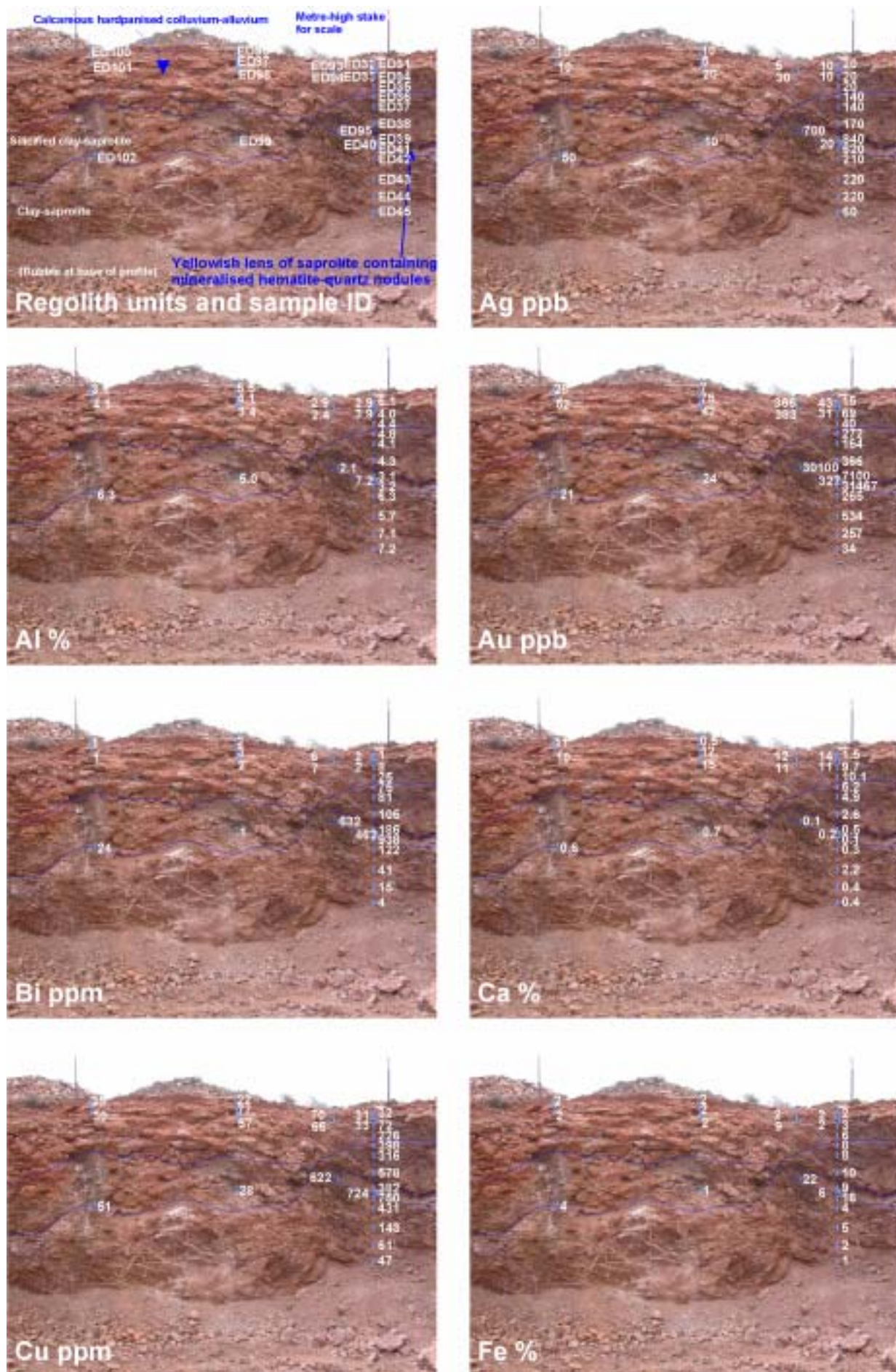


Figure 17: Distribution of selected elements in the northern pit wall of Ian's Mine.



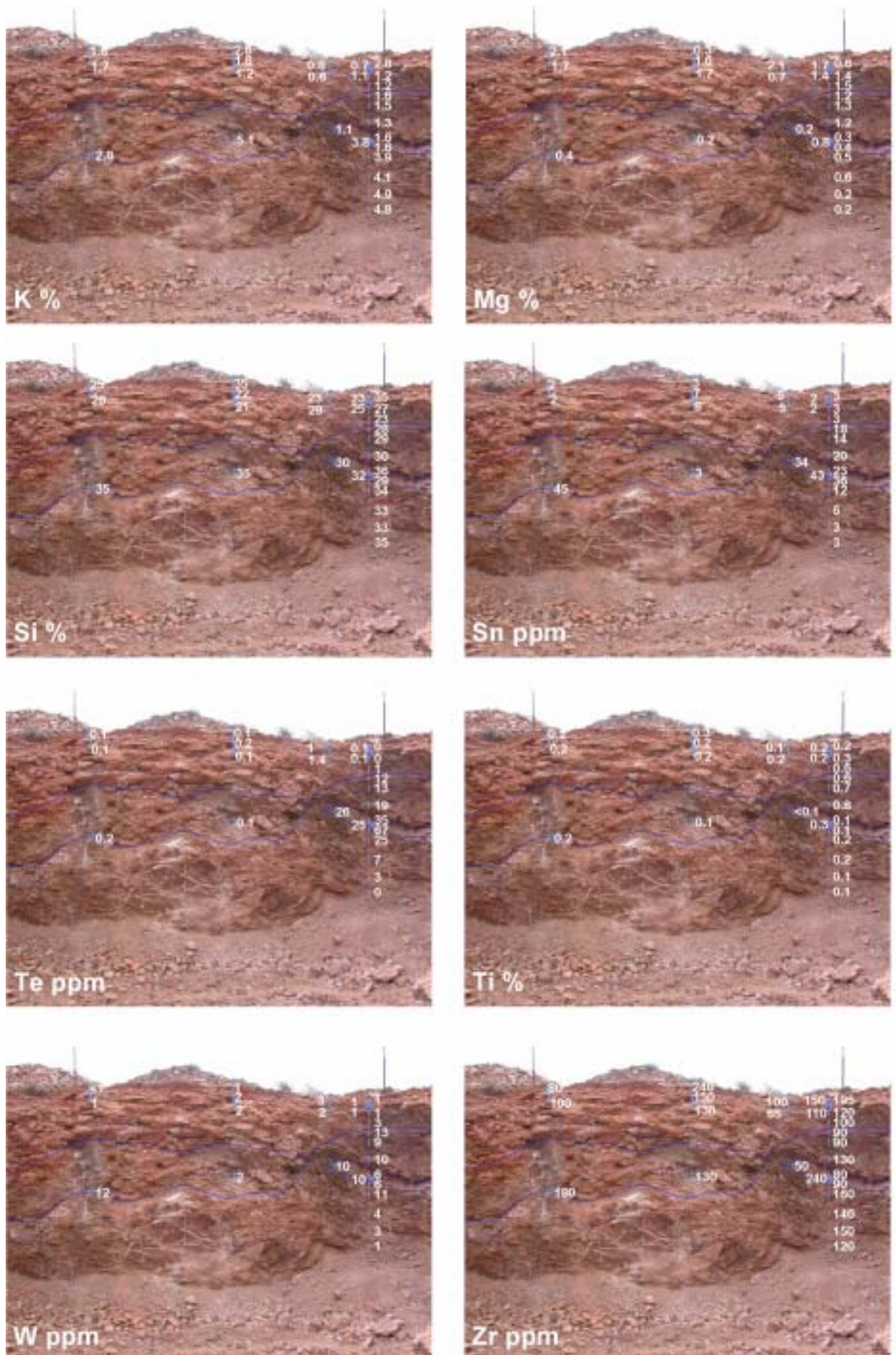


Figure 17 (continued): Distribution of selected elements in the northern pit wall of Ian's Mine.

## 4.7 Soil geochemistry

### Gold

Gold concentrations in soil range from <0.5 to 43 ppb (mean of 3.5 ppb, Figure 18a). The erosional areas appear to have the highest Au concentrations (Figure 18b) especially near Ian's Mine, and are correlated with Ca when Ca concentrations exceed about 1% indicating an association with calcrete (Figure 18c). Therefore, calcareous samples should be considered separately in any regional survey as they are likely to contain higher Au concentrations than samples with low carbonate. Similarly, samples low in carbonate should have lower Au anomaly thresholds. There is some dispersion of Au into the depositional areas with concentrations here of the order of 2-3 ppb but the dispersion is limited to 200 m downslope of known occurrences of mineralization, and thereafter is indistinguishable from background Au concentrations. With respect to elements associated with mineralization, the samples with the two highest Bi concentrations and highest Cu concentration are also anomalous in Au although Fe, Ag, Sn, Te and W concentrations are relatively low in comparison.

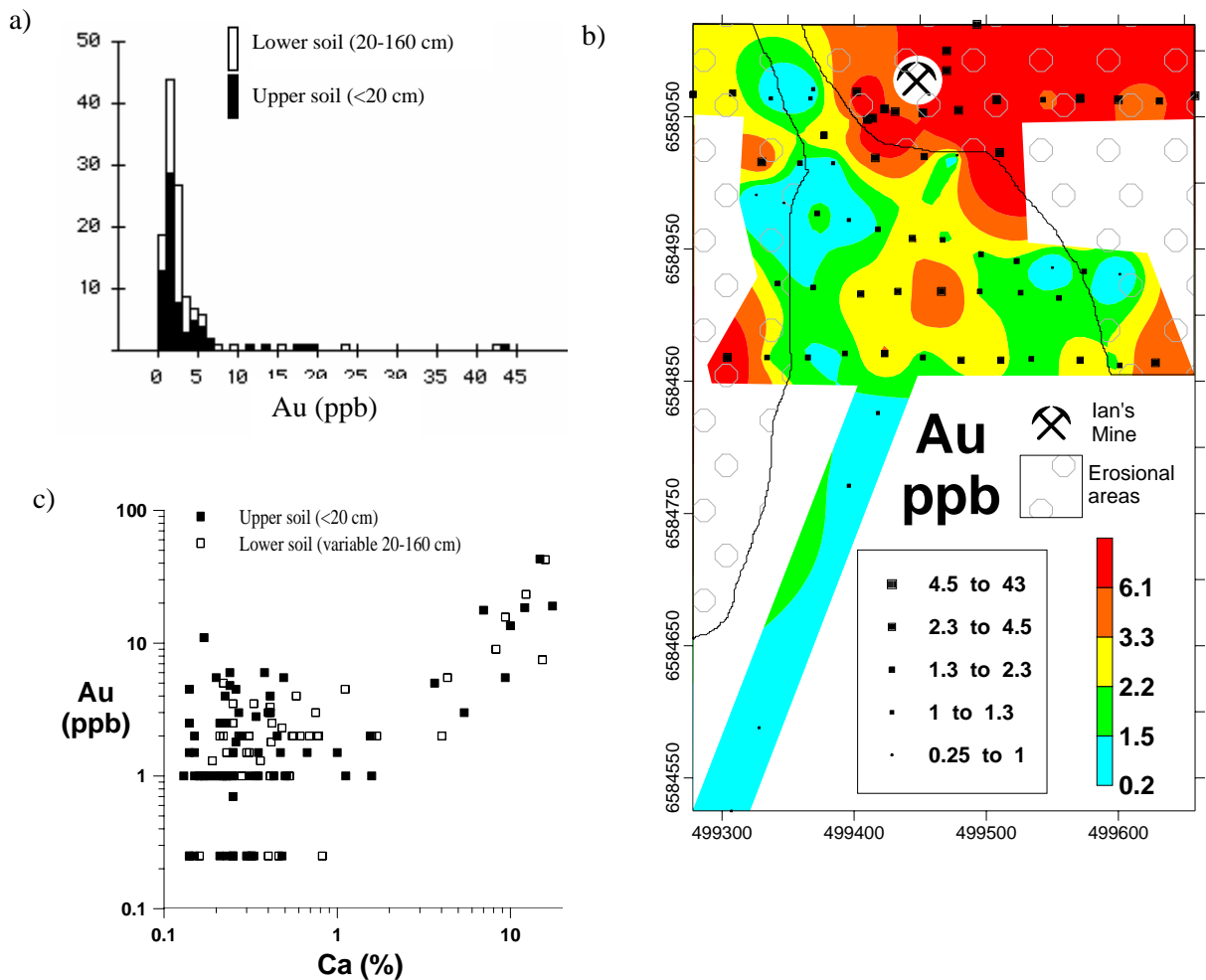


Figure 18: Gold in soils: a) histogram of Au data. Lower soil samples are from variable depth between 20-160 cm; b) distribution of soil Au using maximum values at each location; c) Au vs. Ca scatter plot.

## Silver

Silver in soils was determined after a cyanide digest and range in concentration from 5 to 1920 ppb (mean of 44 ppb). Cyanide digests are able to give a lower limit of detection than conventional mixed acid digests. Higher Ag concentrations are found in soils >20 cm depth. Silver appears to have been mobilized and accumulated in the depositional areas downslope of mineralization and be concentrated in the granitoid-rich samples adjacent to the erosional areas to the east and west. The origin of the Ag is unclear but as it is associated with mineralization it may have use in providing a larger regional target than Au which is not as well dispersed.

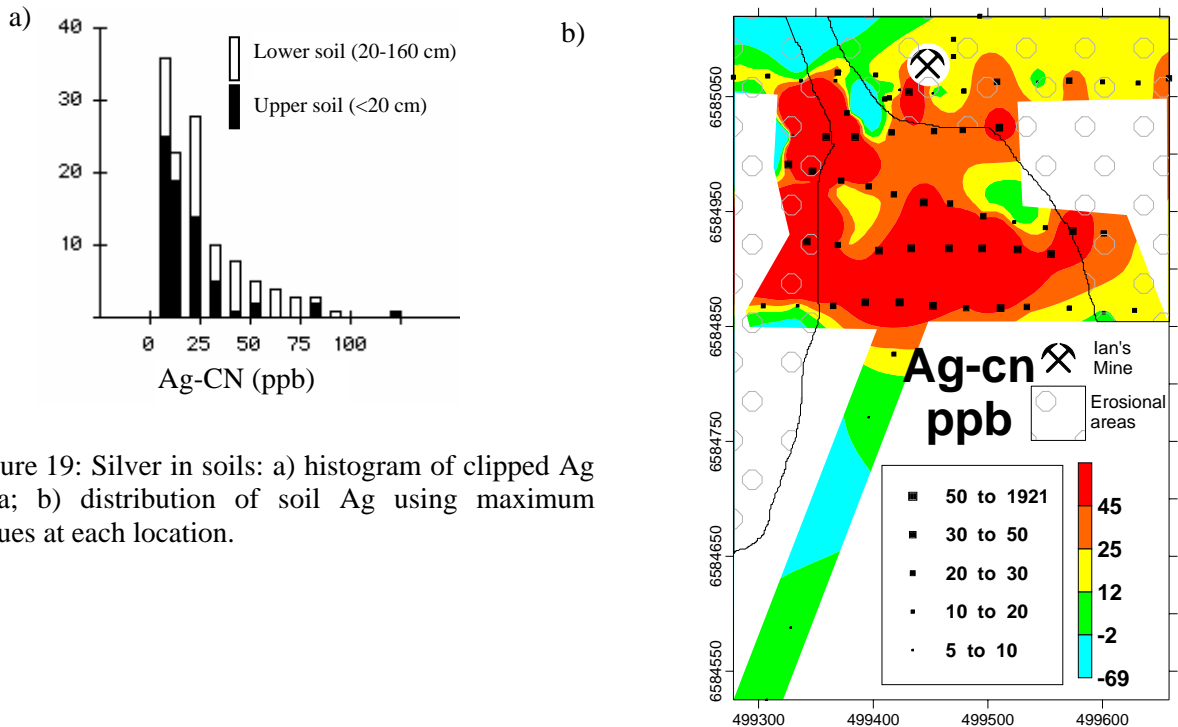


Figure 19: Silver in soils: a) histogram of clipped Ag data; b) distribution of soil Ag using maximum values at each location.

## Aluminium

Aluminium concentrations in soil range from 2 to 8 % (mean of 5 %). The highest Al concentrations are found in the erosional areas and are presumably related to clays, feldspars and muscovite. A “tongue” of Al richer soil extends into the depositional plain and suggests sediment accumulation associated with the hills to the west. Aluminium and Fe are moderately correlated due to co-dilution by quartz and some possible association within clay and Fe oxide minerals.

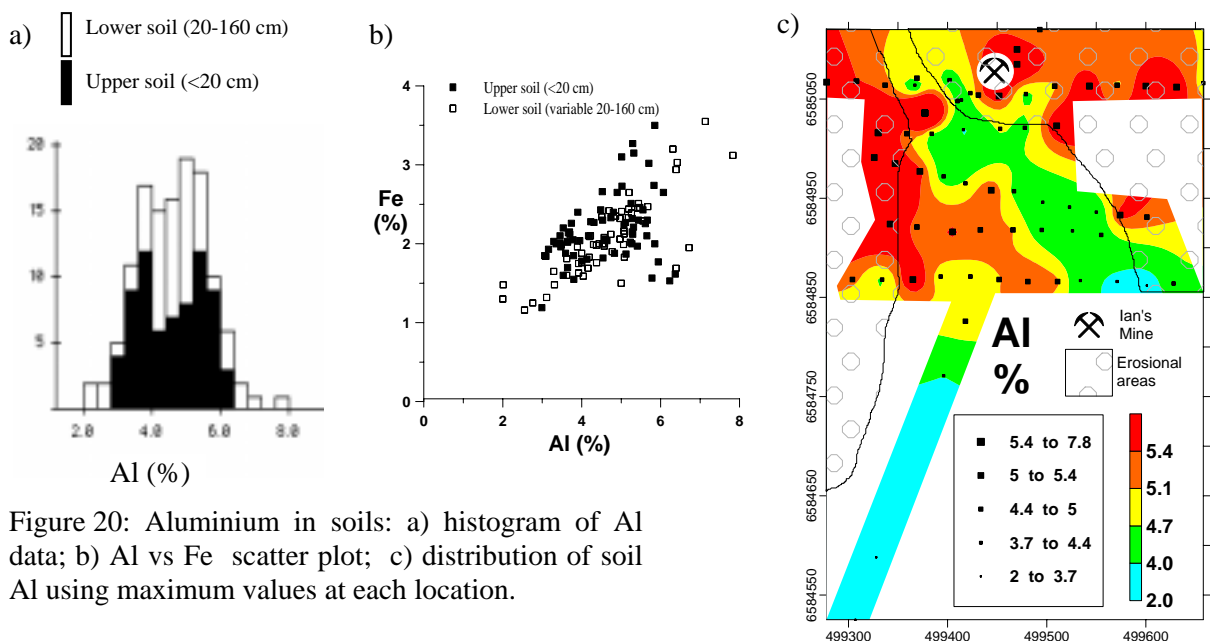


Figure 20: Aluminium in soils: a) histogram of Al data; b) Al vs Fe scatter plot; c) distribution of soil Al using maximum values at each location.

## Bismuth

Bismuth concentrations in soil range from 0.3 to 4.9 ppm (mean of 0.6 ppm) and are especially high around Ian's Mine and on the eastern flank of the erosional area. Dispersion into the depositional area is only moderate indicating it might not be useful for exploration purposes, compared with Ag and to a less extent Au, despite its association with mineralization.

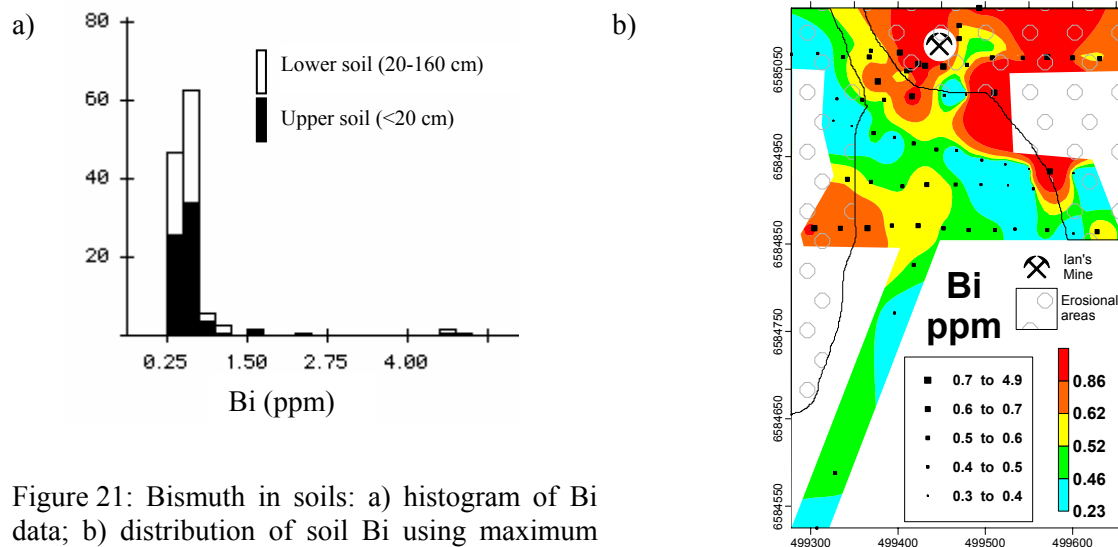


Figure 21: Bismuth in soils: a) histogram of Bi data; b) distribution of soil Bi using maximum values at each location.

## Calcium

Calcium concentrations in soil range from 0.1 to 18% (mean of 1.5%) and are highest in the eastern erosional area; they are most likely related to the presence of carbonate which is notably less abundant in soils to the west, but the reasons for this are unclear. The presence of basic dykes may yield more Ca to the soils but there is no evidence to suggest that they are more prevalent or have greater exposure on the eastern flank. Gypsum, while abundant in the east and south faces of Ian's Mine, was not noted in soil samples. Calcium (in carbonate) has a diluting effect on many elements but its relationship with Cu-CN is similar to that with Au indicating that "mobile" Cu is present in calcrete.

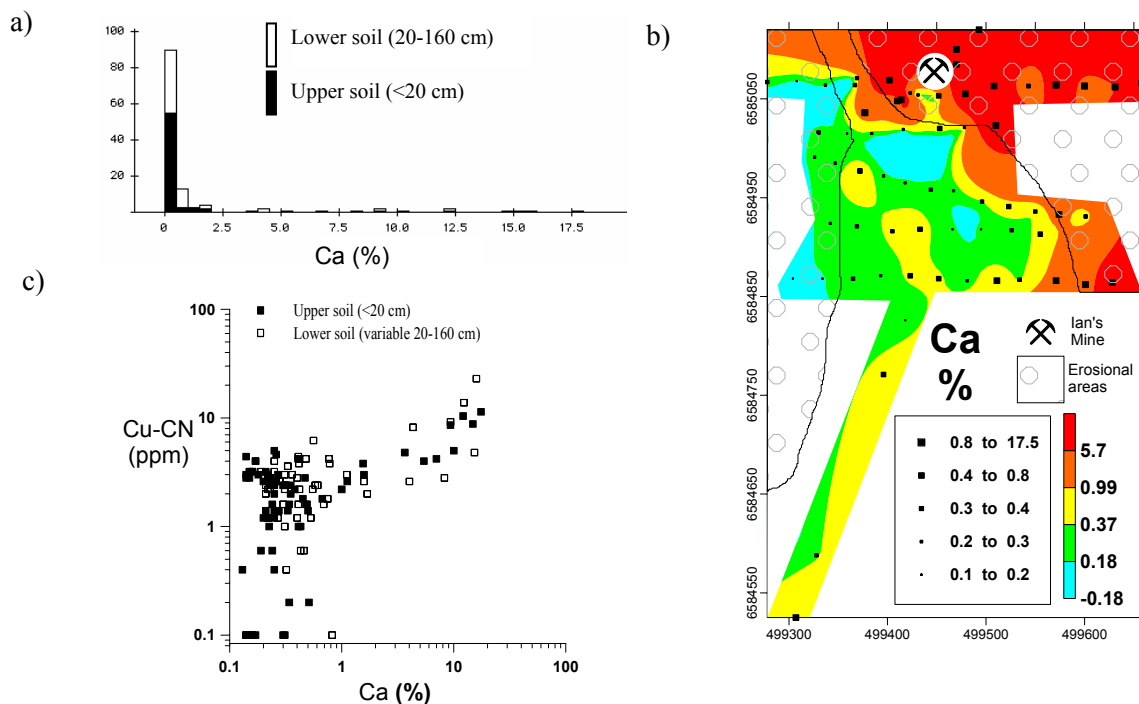


Figure 22: Calcium in soils: a) histogram of Ca data; b) distribution of soil Ca using maximum values at each location; c) Ca vs Cu-CN scatter plot.



## Copper

Copper concentrations in soil range from 7 to 57 ppm (mean of 18.7 ppm). Copper concentrations are highest in the erosional areas and show no preference to being concentrated in the upper or lower soils. Copper is associated with mineralization but there are no particularly high concentrations in soils surrounding Ian's Mine indicating limited use as a pathfinder. Copper shows a weak correlation with Fe (cf Fe).

Cyanide-extractable Cu (Cu-CN) shows a moderate correlation with total Cu but is relatively more concentrated in the depositional areas than total Cu. Cu-CN data is correlated with Mg; the reasons for this are unclear but may be related to the "mobile" Cu present in the calcrete (cf Ca).

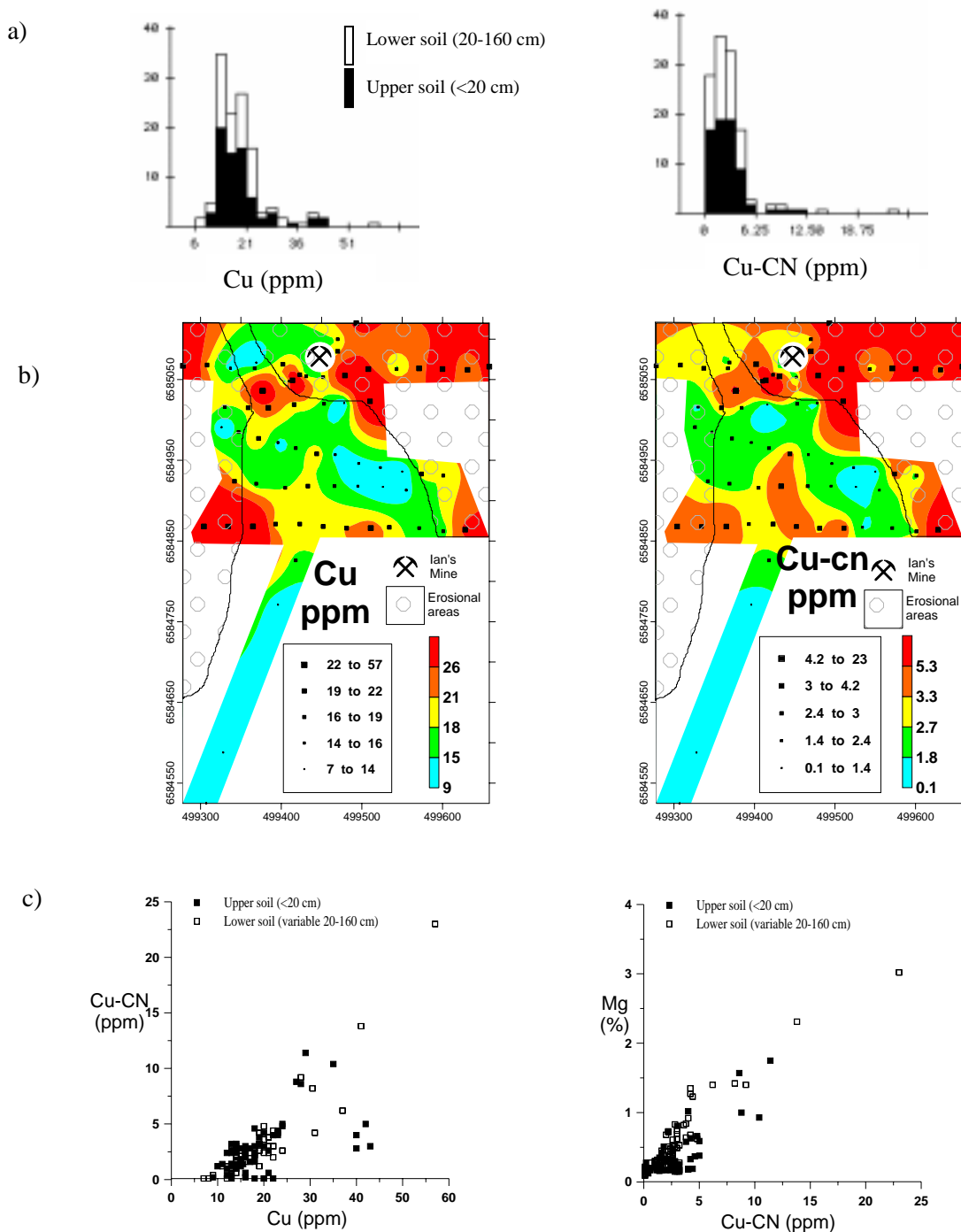


Figure 23: Copper in soils: a) histograms of Cu data; b) distributions of soil Cu using maximum values at each location; c) Cu vs Cu-cn and Cu-cn vs Mg scatter plots.

## Iron

Iron concentrations in soil are generally low ranging from 1.2 to 3.6 % (mean of 2.1 %). Iron concentrations are highest in the erosional area to the east. Moderate to high concentrations are also present in the depositional area. Copper shows a weak correlation with Fe.

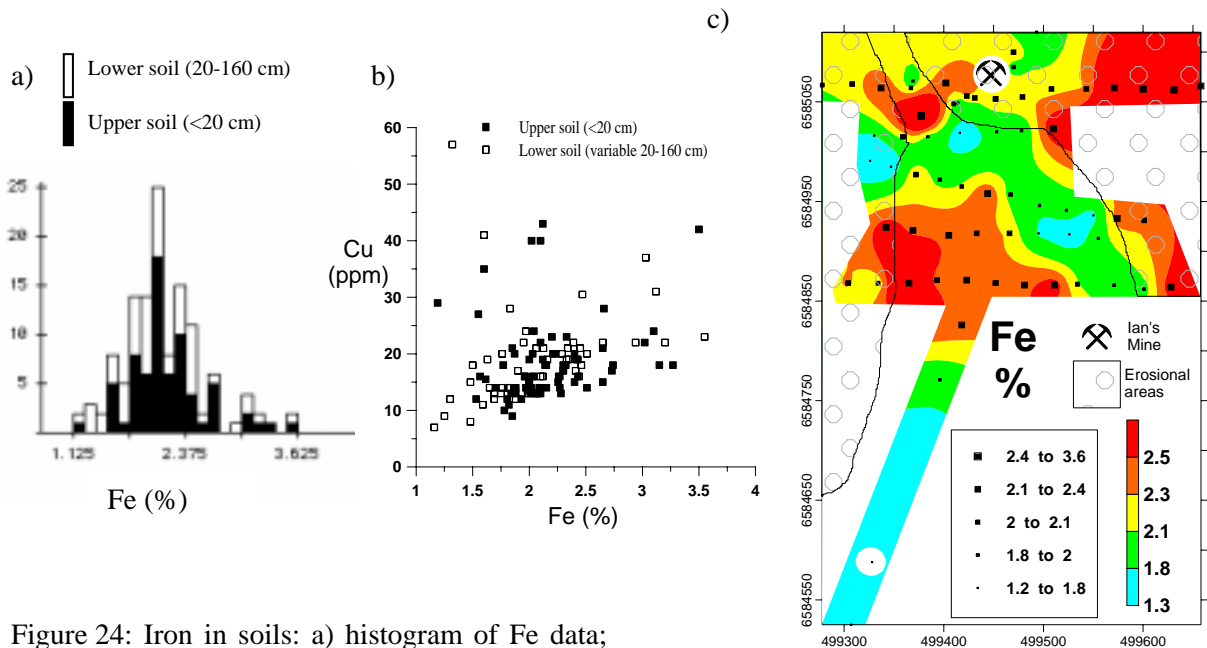


Figure 24: Iron in soils: a) histogram of Fe data; b) distribution of soil Fe using maximum values at each location; c) Fe vs Cu scatter plot.

## Potassium

Potassium concentrations in soil range from 0.9 to 3.7 % (mean of 1.8 %). Potassium is most concentrated in the western erosional area in contrast to Mg and Ca. There is moderate dispersal of K into the depositional area. The origin of K is most likely to be remnant micas and feldspars derived from, and contained within, granite clasts. Where K shows a moderate correlation with Al it reflects co-dilution by Si and possibly the presence of micas or illite although not at sufficient concentrations to be detected in SWIR spectra.

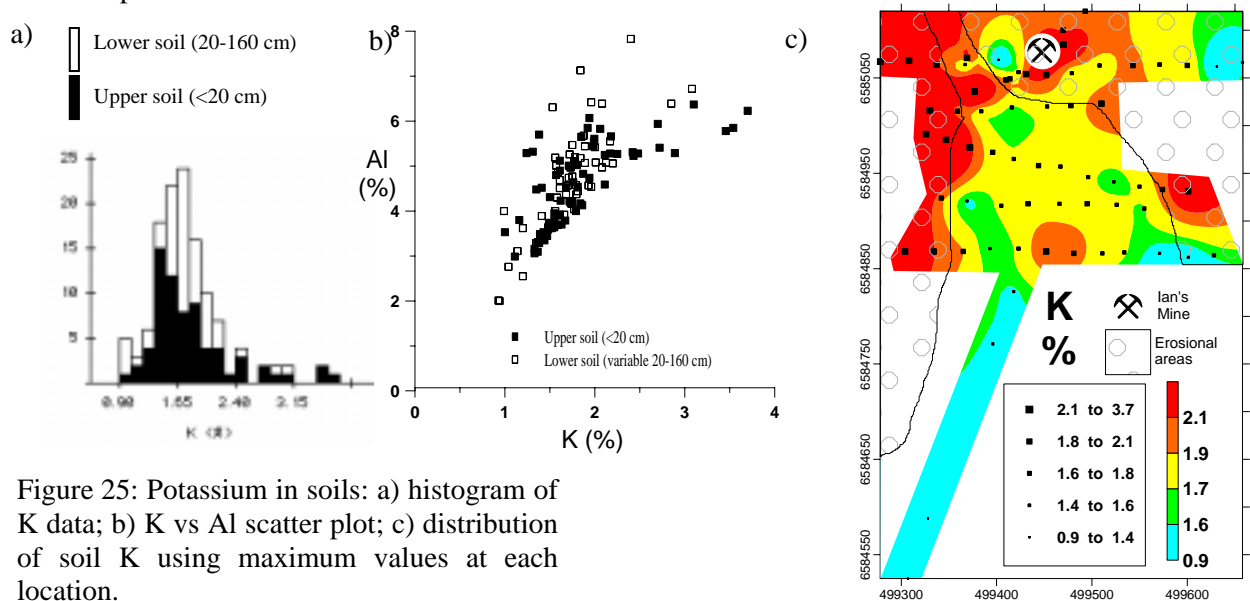


Figure 25: Potassium in soils: a) histogram of K data; b) K vs Al scatter plot; c) distribution of soil K using maximum values at each location.



## Magnesium

Magnesium concentrations in soil range from 0.1 to 3.0 % (mean of 0.47 %). The highest concentrations of Mg occur in the eastern erosional area and, as with Ca, are most likely related to the presence of carbonate which is notably less abundant in soils to the west; the reasons for this are unclear. The weathering of basic dykes may yield more Mg to the soils but there is no evidence to suggest that they are more prevalent or exposed on the eastern flank.

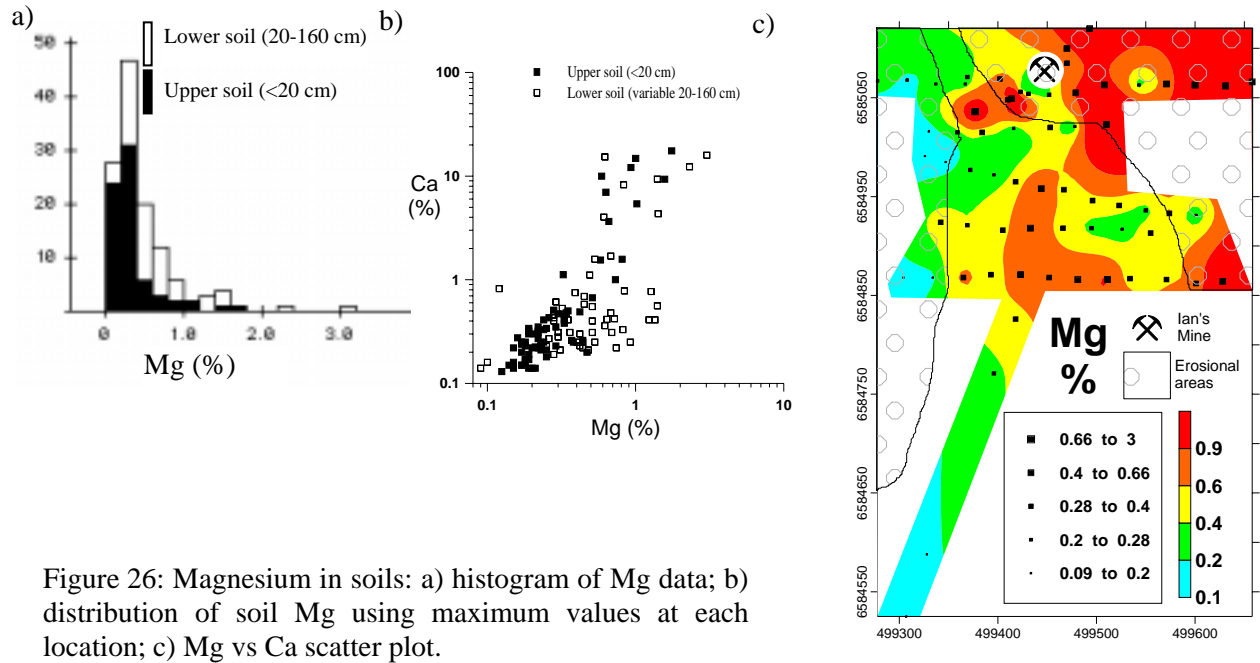


Figure 26: Magnesium in soils: a) histogram of Mg data; b) distribution of soil Mg using maximum values at each location; c) Mg vs Ca scatter plot.

## Silicon

Silicon concentrations in soil range from 19 to 42% (mean of 36%). Higher Si concentrations are found in the lower part of the study area closer to the dune system. Silicon concentrations in the upper soils are presumably due to an aeolian component overprint.

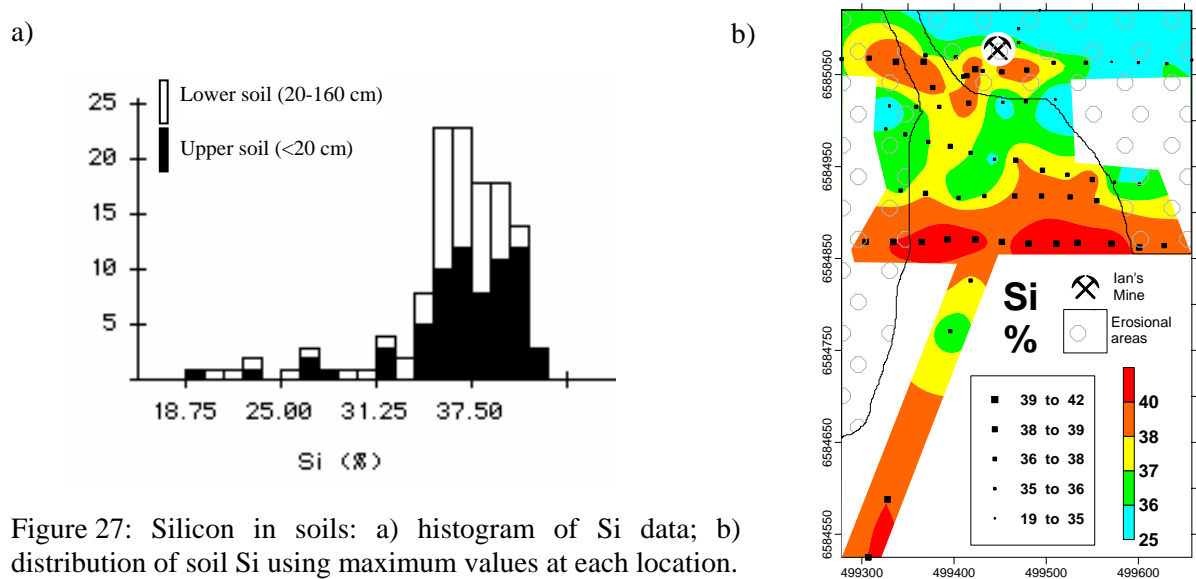


Figure 27: Silicon in soils: a) histogram of Si data; b) distribution of soil Si using maximum values at each location.

## Tin

Tin concentrations in soil range from 0.5 to 27 ppm (mean of 2.2 ppm). Tin is associated with mineralization but the highest concentrations in soils are patchy throughout the study area. The highest concentration (27 ppm) occurs in the valley with surrounding Sn concentrations 3 ppm or below. Detrital fragments of native Sn or cassiterite shed from mineralization may account for the observed distribution since other pathfinders are not anomalous. An abandoned Sn mine is located on the southern side of South Lake, immediately south of Earea Dam Prospect, confirming that Sn is anomalous in this area.

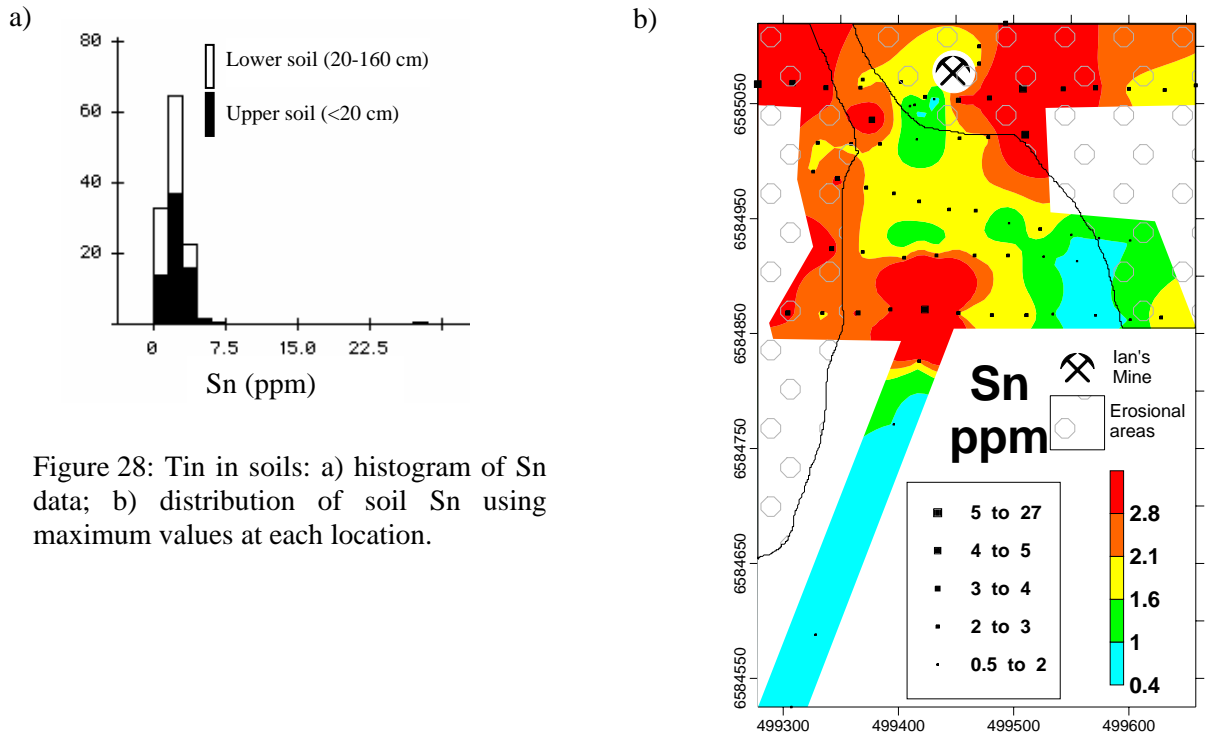


Figure 28: Tin in soils: a) histogram of Sn data; b) distribution of soil Sn using maximum values at each location.

## Tellurium

Tellurium concentrations in soil range from 0.1 to 0.2 ppm. The slightly higher concentrations (0.2 ppm) of Te are mostly found on the easterly hill. Tellurium is associated with mineralization with concentrations in some samples exceeding 30 ppm. However, since soil concentrations are mostly at or close to detection its dispersion characteristics or its use in exploration cannot be determined. .

## Titanium

Titanium concentrations in soil range from 0.14 to 0.42 % (mean of 0.26 %). Its abundance is strongly related to Fe suggesting the presence of ilmenite or a Ti association with Fe oxides.

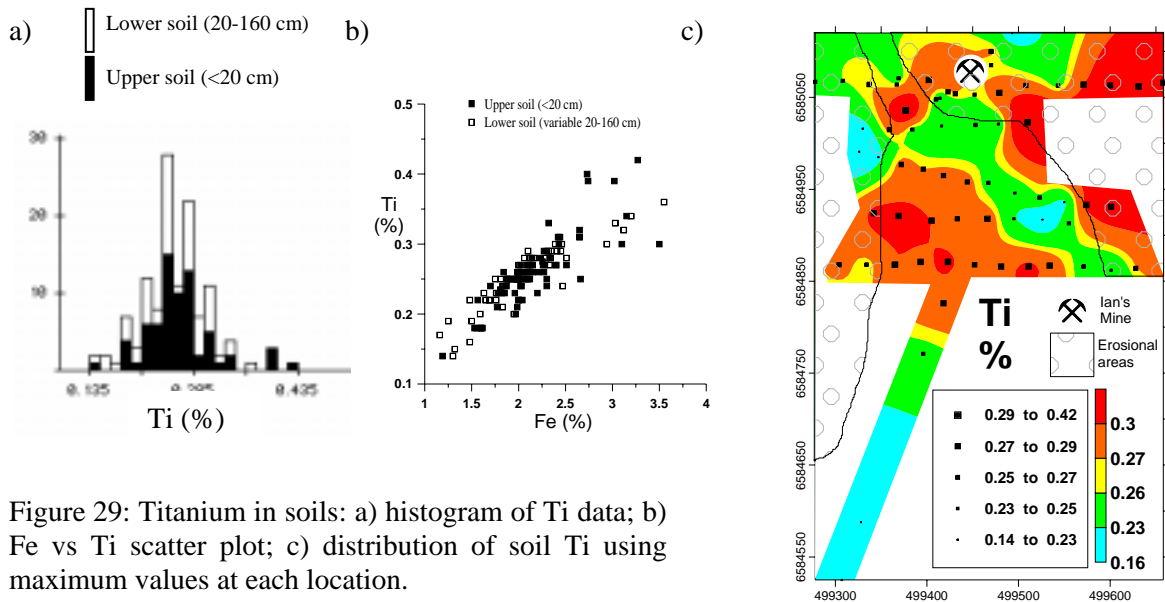


Figure 29: Titanium in soils: a) histogram of Ti data; b) Fe vs Ti scatter plot; c) distribution of soil Ti using maximum values at each location.

## Tungsten

Tungsten concentrations in soil range from 0.25 to 11.5 ppm (mean of 1.8 ppm). Tungsten in soil is predominantly concentrated in the valley floor in sub-surface soils (Figure 30). While W is associated with mineralization, concentrations rarely exceed 15 ppm. It is surprising, therefore, to find concentrations in the soil in excess of a few ppm given dispersion and dilution by background material. There is a possibility that the W found in the valley is contamination from the auger bit used during the collection of hardpanised samples. Shallower soil samples collected without the auger do not show the anomalism. Further work is required since if the W data are genuine then W may be an important pathfinder in sub-soils in this environment.

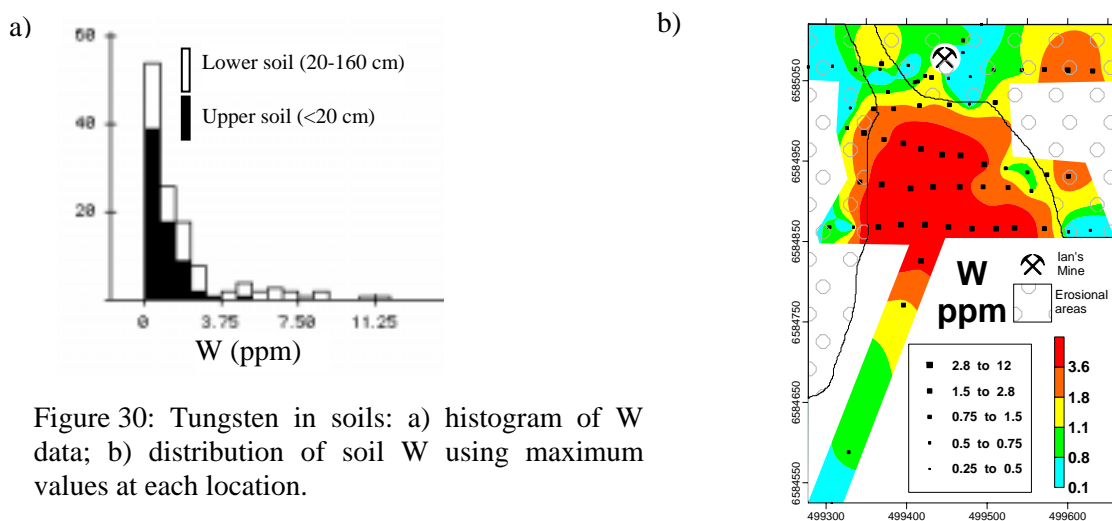


Figure 30: Tungsten in soils: a) histogram of W data; b) distribution of soil W using maximum values at each location.

## Zirconium

Zirconium concentrations in soil range from 110 to 380 ppm (mean of 247 ppm). There appears to be a residual accumulation of Zr in the upper soil (280 ppm, <20 cm depth) compared with deeper soil (210 ppm, to 160 cm). Zirconium is probably mostly present as zircon. The highest Zr concentrations in the soil are located in the erosional areas.

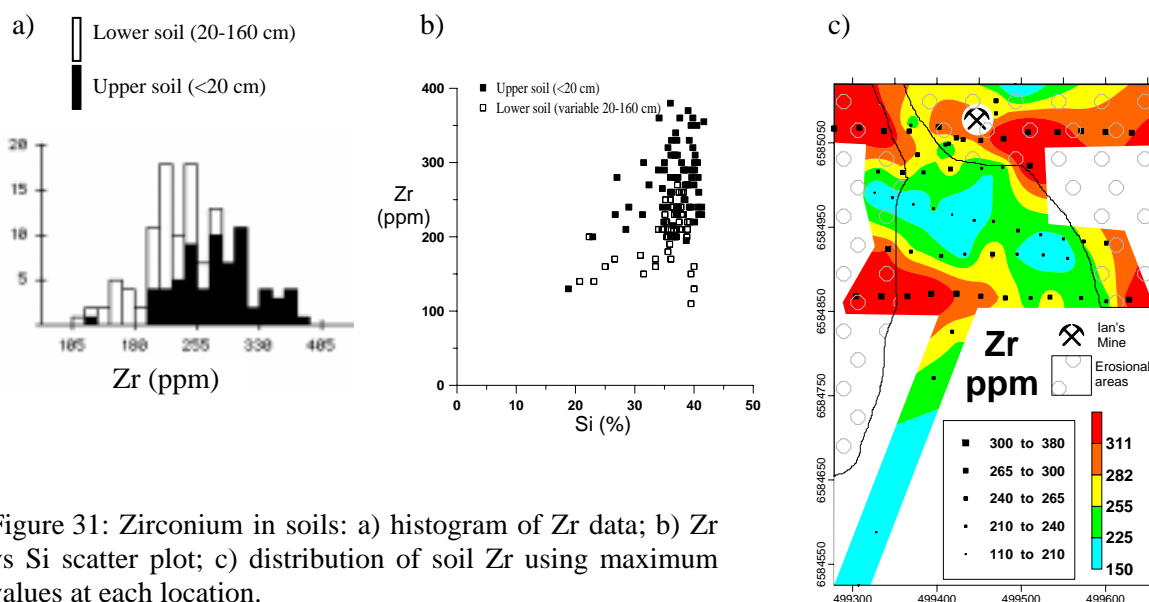


Figure 31: Zirconium in soils: a) histogram of Zr data; b) Zr vs Si scatter plot; c) distribution of soil Zr using maximum values at each location.

## 4.8 SIZE FRACTION ANALYSIS

Five samples were selected (based on their Au content) to determine the distribution of selected elements in certain size fractions (<75, 75-180, 180-250, 250-500, 500-710, 710-1000, 1000-2000, >2000  $\mu\text{m}$ ). One was a non-calcareous soil (ED269) from the valley down slope of mineralization and the others were calcrete samples (ED21, ED93, ED114 and ED231) taken from near mineralization. Most bulk samples were dominated by coarse material (>2 mm; Figure 32). For sample ED269, six size fractions were analysed for selected elements (<75, 75-180, 180-250, 250-500, 500-710, 710-1000, 1000-2000  $\mu\text{m}$ ); and for the calcrete samples, three size fractions (<75, 75-180, >2000  $\mu\text{m}$ ) representing the most abundant particle sizes were selected.

Sample ED269 had minor coarse fraction (>1000  $\mu\text{m}$ ) material and instead was dominated by wind-blown sand in the 75-500  $\mu\text{m}$  size class. Gold, Ag, Al, Bi, Ca, Cu, Fe, Mg, Sn, Ti, W and Zr are most concentrated in the clay-rich fraction (<75  $\mu\text{m}$ ); note that this includes some of the elements (Au, Ag, Bi and Sn) associated with mineralization. The 75-500  $\mu\text{m}$  size fractions had slightly higher Si content confirming their domination by quartz particles. Quartz was also present in the coarser material but had more angular quartz and bedrock fragments locally-derived by sheetflow processes.

For the calcrete samples, Au was marginally more concentrated in the coarse fraction (>2 mm) compared with the fine fraction (<75  $\mu\text{m}$ ) although sample ED93, with 5170 ppb Au, clearly had some discrete Au grains present. Silver, Cu, and Mg concentrations were also lowest in the 75-180  $\mu\text{m}$  where Si concentrations were highest suggesting dilution. Elements most concentrated in the fine fraction include Al, Fe, Sn, Ti, W and Zr suggesting an affinity with clay minerals.

The size fraction study for soils suggests that there is some benefit in collecting and analysing the fine fraction (<75  $\mu\text{m}$ ) in preference to coarser fractions, for exploring for Au. Dilution by windblown and detrital quartz is a concern for exploration in this area. Field observations suggest coarse size fractions (>2 mm) are not recommended unless very coarse rock lag is removed (*e.g.*, by sieving out the >6 mm fraction) from the sample prior to collection, otherwise samples will be dominated by one or two rock clasts.

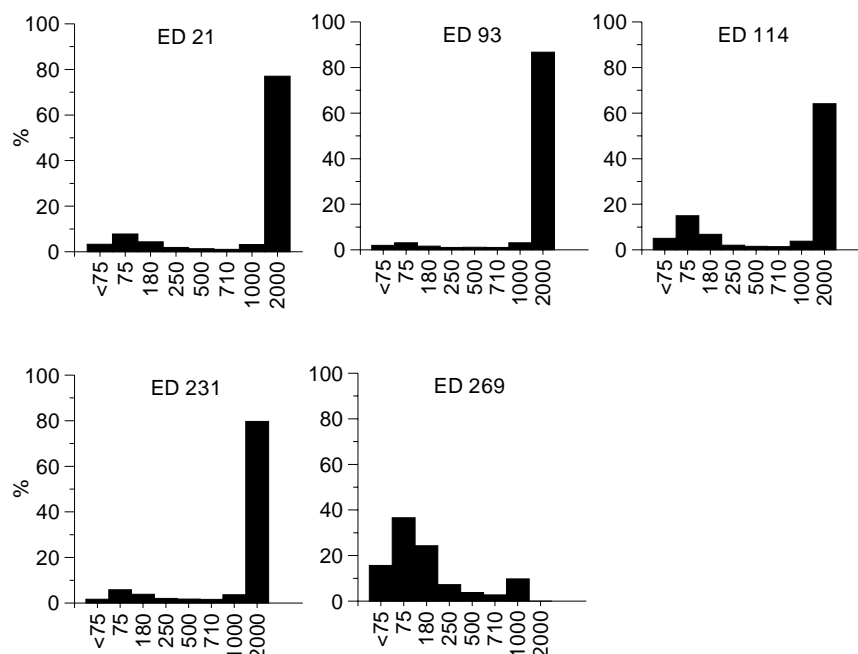


Figure 32: Size fraction analysis (<75  $\mu\text{m}$  to >2000  $\mu\text{m}$ ) for 5 selected samples: ED21 – calcrete containing rock fragments (partially weathered pyroxene-hornblende granulite and granitoids); ED93 – friable nodular calcrete with rock fragments; ED114 – laminar and platy calcrete containing rock fragments; ED231 – friable, platy and nodular calcrete containing rock fragments; ED269 – clay-rich red soil from valley floor. The calcrete samples can be viewed in Figure 8.

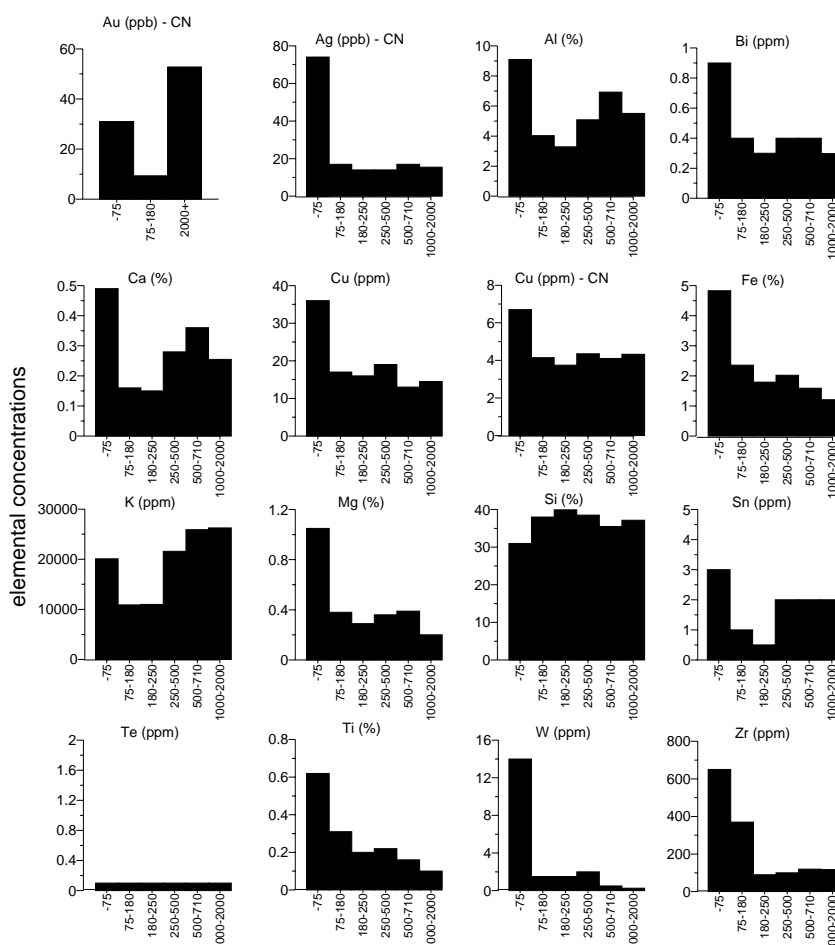


Figure 33: Distribution of selected major and trace elements in size fractions (<75  $\mu\text{m}$  to 2000  $\mu\text{m}$ ) of sample ED269.

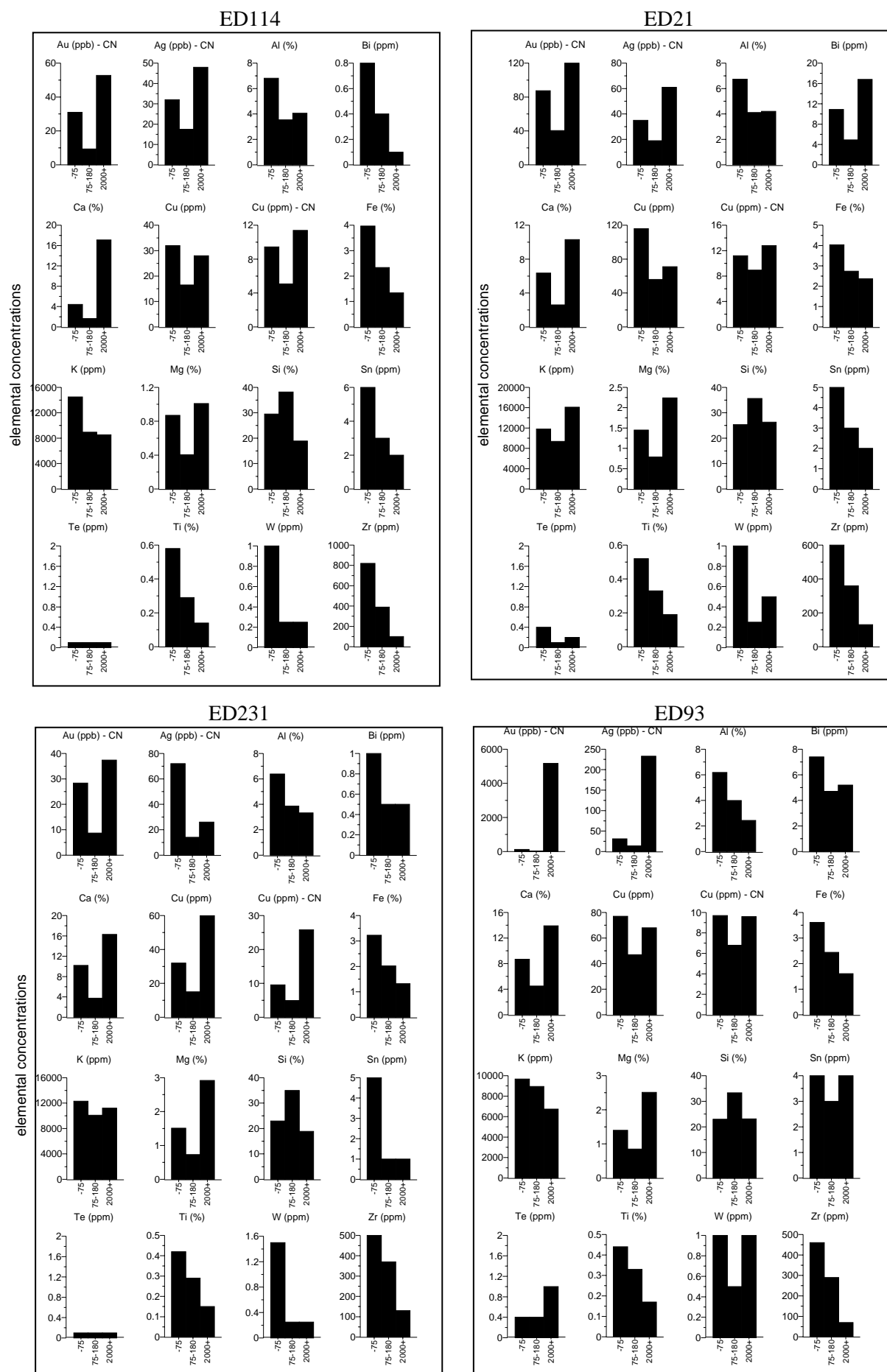


Figure 34: Selected elemental distribution in three size fractions ( $<75\ \mu\text{m}$ ,  $75\text{-}180\ \mu\text{m}$  and  $>2000\ \mu\text{m}$ ) for samples ED114, ED21, ED231 and ED93.



## 5 CONCLUSIONS

Earea Dam Goldfield is dominated by hills of partially-weathered rock (gneiss and mafic dykes) surrounded by depositional areas of thin (<5 m) colluvium-alluvium and deeper sand dunes. Specific investigations at Ian's Mine at Earea Dam, indicated that weathering was shallow with saprolite containing corestones of saprock (gneiss) occurring within 4 m of the surface. Mineralization is associated with quartz-hematite veins that dip into the gneiss at a shallow angle. At Ian's Mine, remnants of these veins (as gravels) can be traced through the saprolite-saprock to calcrete and thin soil at the surface and provide an opportunity to examine elemental dispersion from mineralization directly into the soil. Geochemically, the quartz-hematite gravels are rich in Au (some visible) and a number of associated elements (Ag, Bi, Cu, Sn, Te, U and W). The absence of a significant supergene horizon, the narrowness of the veins and/or the resilient nature of the quartz-hematite gravels themselves maybe important factors for the lack of significant dispersion plumes in the depositional plain downslope of Ian's Mine.

## 6 IMPLICATIONS FOR EXPLORATION

1. Landsat TM data and aerial photography were used to construct the regolith landform map which in turn was used to understand landform relationships and estimate depth of cover.
2. Gravels of mineralized quartz-hematite veins provide poor vectors to the vein source since they are only weakly physically dispersed downslope. They appear to be locked within massive and laminar hardpanised material including calcrete. Detrital material is diluted by poorly-mineralised material from surrounding hills.
3. Evidence for chemical dispersion is weak and appears to be confined to within 200 m of Ian's Mine. Close to their source, the gravels are locked within massive and laminar calcretes and there is little evidence of hydromorphic dispersion of Au into calcretes above mineralization as demonstrated by their poor correlation.
4. Multi-element geochemistry (Ag, Bi, Cu, Sn, Te, U and W) in soils may be regionally effective in this area. However, locally, from Ian's Mine, only Ag appears to be reasonably dispersed and may provide an additional target element to Au. Tungsten may also be effective but needs to be investigated further.
5. There is some benefit in collecting and analysing the fine fraction (<75 µm) in preference to coarser fractions, to remove windblown quartz, barren detrital gravels and coarse rock lag.

## 7 SUMMARY

Construction of a regolith-landform map and geochemical survey were undertaken at the Earea Dam Goldfield in the Gawler Craton, South Australia. Erosional and depositional areas were identified and a geochemical survey, comprised of profile sampling, soil sampling and augering was conducted centred around Ian's Mine at Earea Dam. Gold mineralization was related to sub-cropping quartz-hematite veins at Ian's Mine but, despite Au-rich gravels cemented in surficial calcrete, geochemical dispersion was limited to a couple of hundred metres downslope. Silver, Bi, Cu, Sn, Te, U and W are associated with mineralization but Ag appears to be the only element that is significantly dispersed in soil and may provide a broader target than Au for exploration purposes.

## 8 ACKNOWLEDGEMENTS

The following are thanked for their support and expertise in preparation of this report: A.J. Cornelius for preparing the GIS and processing the ASTER data. R. Hewson for acquiring and crosstalk-correcting the ASTER data. J. Wilson (Figure 2), T. Naughton (Figure 3 and Figure 9), and A.J. Cornelius (Figure 10) for help with diagrams; D.J. Gray, R.A. Anand and C.R.M. Butt gave valuable comments on earlier drafts of this report. CRC LEME is supported by the Australian Cooperative Research Centres Program.

## 9 REFERENCES

- Brown, H.Y.L., 1908. Record of the Mines of South Australia. Fourth Edition. 381 pp.
- Circosta, G. and Gum, J., 1989. Geological investigation. Mining leases 5342 and 5361, Earea Dam, South Australia. Report by Tarcoola Gold Ltd. In Open File Envelope No 8062. South Australia Department of Mines. Unpaginated.
- Crettenden, P.P. and Fradd, W.P., 1992. Geological and Historical Review of the Earea Dam Goldfield. Mining and Energy Review, South Australia. Department of Mines. pp 81-83.
- Daly, S.J., Benbow, M.C. and Blisset, A.H., 1979. Archaean to Early Proterozoic geology of the northwestern Gawler Craton. In Parker, A.J. (Compiler), Symposium on the Gawler Craton, Extended Abstracts. Geol. Soc. Australia., Adelaide. pp 16-19.
- Eggleton, R.A., (Editor) 2001. The Regolith Glossary. CRC LEME , Perth, Australia. 144 pp.
- Hewson R., Cudahy T. and Shoji, M., 2003. Evaluation and processing of satellite ASTER image data to generate accurate, seamless geological maps for regional surveys. CSIRO Exploration and Mining Report No. 1084F. 63 pp.
- Lintern, M.J., (Compiler) 2004. The South Australian Regolith Project Final Report – Summary and Synthesis. CRC LEME Open File Report 156. 41 pp + 81 pp Appendices
- Lintern, M.J. and Sheard, M.J., 1998. Regolith studies related to the Challenger Gold Deposit, Gawler Craton, South Australia. Geochemistry and stratigraphy of the Challenger Gold Deposit. CRC LEME Restricted Report 78R, 2 Volumes. 95 pp + Appendices (un-paginated). Reissued as CRC LEME Open File Report 78, 1999.
- Lintern, M.J., Sheard, M.J. and Gouthas, G., 2000. Regolith studies related to the Birthday Gold Prospect, Gawler Craton, South Australia. CRC LEME Open File Report 79. 201 pp.
- Lintern, M.J., Sheard, M.J. and Gouthas, G., 2002. Preliminary regolith studies at ET, Monsoon, Jumbuck, South Hilga and Golf Bore Prospects, Gawler Craton, South Australia. CRC LEME Open File Report 115, 2 Volumes. 43 pp + 262 pp Appendices.
- Tapley, I. J. and Gozzard, J. R., 1992. Regolith-Landform Mapping in the Lawlers District. Report 1: Aerial photographic interpretation and Landsat Thematic Mapper processing for mapping regolith-landforms (Volumes 1 and 2). CSIRO IMEC Division of Exploration Geoscience Restricted Report 239R

## 10 APPENDICES

# **APPENDIX 1**

# Mason Geoscience Pty Ltd

*Petrological Services for the  
Minerals Exploration and Mining Industry*

ABN 64 140 231 481

ACN 063 539 686

Postal: PO Box 78 Glenside SA 5065 Australia

Delivery: 141 Yarrabee Rd Greenhill SA 5140 Australia

Ph: +61-8-8390-1507 Fax: +61-8-8390-1194

e-mail: masongeo@ozemail.com.au

## **Petrographic Descriptions for Eight Regolith Samples (mainly Earea Dam Goldfield, Gawler Craton, South Australia)**

REPORT #                    **2809**

CLIENT                    **CSIRO / CRCLEME**

ORDER NO                **Letter, M. Lintern, 3 December 2002**

CONTACT                **Mr Melvyn Lintern**

REPORT BY              **Dr Douglas R Mason**

SIGNED

**for Mason Geoscience Pty Ltd**

DATE                    **9 December 2002**

# Petrographic Descriptions for Eight Regolith Samples (mainly Earea Dam Goldfield, Gawler Craton, South Australia)

## SUMMARY

### 1. Rock Samples

- Eight rock samples representing regolith and associated basement rocks from the Earea Dam Goldfield (Mulgathing Complex, Gawler Craton, South Australia) have been studied using routine petrographic methods.

### 2. Brief Results

- *A summary of rock names and mineralogy is provided in TABLE 1.*
  - *Primary rock types*
    - **Pyroxene-hornblende granulite** is identified in two samples (ED11-1, ED21-1). It formed by complete recrystallisation of precursor basic rock (probably basic igneous rock) under high P-T conditions (granulite facies of regional metamorphism) to form a fine-grained granoblastic assemblage of plagioclase + pyroxene + hornblende + minor opaques (including magnetite). Subsequent low-grade retrogressive metamorphism in the greenschist facies resulted in complete replacement of pyroxene by actinolite + trace opaques (magnetite), as well as filling of thin brittle fracture sets by actinolite.
    - **Felsic crystalline rocks** are composed of inequigranular, massive to weakly foliated assemblages dominated by plagioclase, quartz and K-feldspar (orthoclase microperthite), accompanied by traces of biotite, opaques and zircon. They are considered to represent felsic bands, veins or intrusive bodies of broadly leuco-granitoid composition, developed in the high-grade metamorphic terrain. Some samples display retrogressive alteration (quartz + sericite/muscovite) which might belong to the retrogressive alteration event recorded in the mafic granulites, or possibly reflect alteration associated with a veining and mineralisation event (see next).
    - **Quartz-sulphide-gold vein** (sample ED95-1) formed as a space-filling hydrothermal vein deposit composed of granular quartz + sulphide(s) (including pyrite) + minor biotite + trace native gold. Adjacent quartzo-feldspathic host rock suffered strong phyllic-type alteration to form the new assemblage of quartz + sericite. Post-vein deformation has caused partial recrystallisation of the vein quartz with associated destruction of primary fluid inclusions. Strong selective pervasive oxidation in the supergene environment generated abundant microgranular hematite after the precursor sulphide(s).
  - *Weathering and regolith evolution*
    - **Regolith materials** are represented by sandy clastic components (mainly quartz and feldspars, with trace hornblende, opaques and rutile, as well as fragments of the felsic and mafic lithic precursors from which these crystalline materials were derived) firmly bound by cements of ferruginous clays (claycrete) and/or calcite (calcrete). Stages of evolution of the regolith are recorded in microtextural relationships between the low-temperature cements. Initial cementation by ferruginous clays resulted in firm binding of the clastic materials. Fine-grained calcite formed a later cement, and latest opaline silica and fibrous chalcedony was deposited in small amount as thin pore linings and fillings (sample ED21-1).
-

**TABLE 1: SUMMARY OF ROCK NAMES AND MINERALOGY**

SAMPLE	ROCK NAME	MINERALOGY*			
		Primary**	Alteration***	Veins	Weathering***
1. ED70-1	Calcrete cemented ferruginous claycrete	Qtz, pla, Kf, hbl, opq	-	-	FeCla; Cal
2. ED11-1	Partly retrogressed pyroxene-hornblende granulite	-	Pla, hbl, opq (?mt); Act, opq(?mt)	-	Goe
3. ED102-1	Weathered, partly retrogressed, biotite granitoid	Pla, bio?, zir	qtz, Mus/ser, bio?, ana, zir?	-	Goe, hem
4. ED21-1	Weakly weathered, partly retrogressed, pyroxene-hornblende granulite	-	Pla, hbl, opq(?mt); Act, opq(?mt)	-	Goe
	Sandy calcrete	Qtz, pla, Kf	-	-	FeCla; Cal, ccy
5. ED17-1	Weakly weathered foliated leuco-granitoid (biotite quartz monzonite)	Pla, qtz, Kf, bio, opq, zir	-	-	Goe, hem
6. ED241-1	Sandy ferruginous claycrete	Qtz, Kf, pla, hbl, opq	-	-	FeCla
7. ED95-1	Oxidised quartz-sulphide(-gold) vein	-	-	Qtz, bio, py, gld	Hem, cla, goe
	High-intensity phyllic (quartz-sericite) altered host rock	-	Qtz, ser	-	Goe
8. TE104	Calcreted sandy ferricrete	Qtz, opq, rut, hbl	-	-	FeCla, cal

**NOTES:**

\*: Minerals are listed in each paragenesis according to approximate decreasing abundance.

\*\***: Only primary minerals currently present in the rock are listed. Others may have been present, but are altered.**

\*\*\*: Earlier parageneses are separated from later parageneses by a semicolon.

**Mineral abbreviations:**

Act = actinolite; ana = anatase; bio = biotite; cal = calcite; ccy = fibrous chalcedonic silica; cla = undifferentiated clays; FeCla = ferruginous stained clay; gld = native gold; goe = goethite; hbl = hornblende; hem = hematite; Kf = K-feldspar; leu = leucosene; mt = magnetite; mus = muscovite (coarser-grained white mica); opl = opaline silica; opq = undifferentiated opaques (possible mineral in brackets); pla = plagioclase; py = pyrite; qtz = quartz; rut = rutile; ser = sericite (fine-grained white mica); zir = zircon; ?min = uncertain mineral identification; min? = uncertain mineral paragenesis.



## **1 INTRODUCTION**

A suite 8 regolith samples and associated thin sections was received from Mr Melvyn Lintern (CSIRO/CRCLEME, Kensington, WA) on 5 December 2002.

It was indicated that most of the samples originate from the Earea Dam Goldfield, located in the Archaean Mulgathing Complex in the northern part of the Gawler Craton of South Australia. Brief hand specimen rock names were provided for each sample. Particular requests were:

- i) To prepare a petrographic description (code PETRO 2) for each sample.
- ii) To provide the results promptly.

Preliminary results were provided by email to Mr Lintern on 8 December 2002. This report contains the full results of this work.

## **2 METHODS**

At Mason Geoscience Pty Ltd conventional transmitted polarised light microscopy was used to prepare the routine petrographic descriptions.

The thin sections lacked coverslips, so light vegetable oil was used to allow clear viewing. The oil was removed subsequently using light wiping with tissues.

## **3 PETROGRAPHIC DESCRIPTIONS**

The petrographic descriptions are provided in the following pages.

**SAMPLE : 1. ED70-1 (Hardpan with clasts of Kenella Gneiss, Earea Dam Goldfield, SA)**

**SECTION NO : ED70-1**

**HAND SPECIMEN :** The sample represents creamish brown hardpan composed of small (mostly millimetre-sized, up to ~1 cm) angular pale to dark crystal and lithic fragments in a fine-grained brownish cream matrix. Indistinct layering is defined by thinner paler bands in the matrix which enwrap larger lithic fragments.

The matrix effervesces vigorously in reaction with dilute HCl, confirming abundant calcite is present.

**ROCK NAME : Calcrete cemented ferruginous claycrete**

**PETROGRAPHY :**

A visual estimate of the modal mineral abundances gives the following:

Mineral	Vol %	Origin
Lithics (qtz, K-feld, plag, hem)	20	Leuco-gneiss fragments
Lithics (amphibole, plag, opaques)	<1	Mafic granulite fragments
Quartz	5	Crystal fragments
Feldspar (plag, K-feld)	1	Crystal fragments
Opagues (?hem/goethite)	Tr	After opaque crystal fragments
Hornblende	Tr	Crystal fragments
Zircon	Tr	Crystal fragments
Ferruginous clays	40	Ferricrete
Calcite	32	Calcrete

In thin section, this sample displays an unsorted matrix supported fragmental texture, with local thin layering defined by more abundant concentration of fine calcite cement.

Lithic fragments are moderately abundant, especially felsic crystalline fragments of leuco-gneiss origin up to ~1 cm in size. They display inequigranular massive crystalline textures composed of sutured recrystallised coarse-grained quartz, large anhedral weakly perthitic orthoclase grains, and anhedral albite-twinning plagioclase grains. Disaggregation of this rock type has produced single crystal fragments of quartz, plagioclase and K-feldspar that range from <0.05 mm up to ~1 mm in size.

Rare lithic fragments of mafic granulite are composed of an equigranular fine-grained assemblage of hematite-stained amphibole grains, plagioclase grains, and minor opaque grains. Disaggregation of this rock type has produced rare small crystal fragments of pleochroic green hornblende.

Zircon is rare, occurring as small angular crystal fragments.

Abundant ferruginous clay materials are fine-grained and orange-brown in colour. It forms thin rinds around some of the lithic fragments, but is more abundant as a dense matrix enclosing lithic and crystal fragments in an indistinct band several centimetres thick. Varied fragmentation of this band is evident.

Calcite is abundant, occurring as a very fine-grained porous cement which mantles fragments (lithic, crystal, and ferruginous claycrete types). Where more abundant, it tends to form dense turbid cryptocrystalline ball-like concentrations that are mantled by colourless very fine-grained calcite.

## INTERPRETATION :

This sample represents near-surface regolith which appears to have evolved through different stages:

1. Protolith of felsic leuco-gneiss and mafic granulite formed in response to high-grade regional metamorphism of precursor rocks.
2. Surficial transport of protolith fragments.
3. Deposition of abundant fine-grained ferruginous clay materials.
4. Partial fragmentation of ferruginous claycrete and deposition of calcite.

**SAMPLE : 2. ED11-1 (Mafic intrusive, Earea Dam Goldfield, SA)**

**SECTION NO : ED11-1**

**HAND SPECIMEN :** The rock chip sample represents a fine-grained massive dark green crystalline rock, which has suffered incipient weathering to produce diffuse orange-brown ferruginous staining from margins inwards.

The sample responds weakly to the hand magnet, suggesting a trace amount of magnetite is present.

**ROCK NAME : Partly retrogressed pyroxene-hornblende granulite**

**PETROGRAPHY :**

A visual estimate of the modal mineral abundances gives the following:

Mineral	Vol %	Origin
Plagioclase (incl. illitic flecks)	50	Metamorphic 1
Hornblende	10	Metamorphic 1
Opakes (incl. magnetite)	2	Metamorphic 1
Actinolite	37	Metamorphic 2 / fracture fillings 2
Opakes	Tr	Metamorphic 2
Goethite	<1	Weathering 3

In thin section, this sample displays a well-preserved massive equigranular granoblastic metamorphic texture, modified by selective retrogressive alteration and subsequent weak weathering.

Plagioclase is abundant, occurring as equant anhedral grains ~0.1-0.2 mm in size. They display their primary polysynthetic twinning, but incipient alteration has generated tiny phyllosilicate flecks (probably illitic clay).

Two types of amphiboles are distinguished:

- Hornblende occurs as equant anhedral grains that are strongly pleochroic from dark khaki green to pale khaki. They represent a Ti-Al-rich hornblende, and clearly formed as part of the granoblastic metamorphic assemblage.
- Pleochroic pale green actinolitic amphibole is abundant, occurring as optically continuous and fine-grained microcrystalline replacements of precursor small equant anhedral ferromagnesian grains that were similar in size to the plagioclase and dark hornblende. None of the precursor phase is preserved, but it most likely was pyroxene (possibly one or both of clinopyroxene and orthopyroxene). A small amount of actinolite also occurs in thin, poorly-defined fractures which define an oriented set through the rock.

Two types of opakes are distinguished:

- Most occurs as small anhedral grains uniformly distributed through the rock. They lie in textural equilibrium with the plagioclase and ferromagnesian minerals, and therefore are interpreted to belong to the principal metamorphic assemblage. The rock responds positively to the hand magnet, suggesting some of these opaque grains are magnetite.

- ii) A trace amount of opaque material occurs as tiny granules located in some of the actinolite. This opaque phase may be magnetite, and clearly belongs to the retrogressive assemblage.

Goethite occurs in minor amount as cryptocrystalline turbid orange-brown material that forms diffuse and locally dense stains, mainly in the actinolite-altered ferromagnesian grains.

#### INTERPRETATION :

This sample represents a basic rock, possibly of igneous origin, which has suffered complete recrystallisation in response to high-grade (granulite facies) regional metamorphism. This generated the equigranular granoblastic assemblage of plagioclase + pyroxene + hornblende + minor opaques (including magnetite). There are no preserved primary minerals or textures of the precursor basic rock, but the uniformly fine grain size of the metamorphic assemblage suggests that the precursor rock also was relatively fine-grained. It may have formed as a lava flow, or as a relatively small intrusive body. It is unlikely to have formed as a large intrusive body.

Subsequent weak retrogressive metamorphism in the greenschist facies caused complete replacement of pyroxene by pale green actinolite and trace opaques (?magnetite). Brittle fracturing affected the rock during this event: this may have encouraged invasion by a small amount of hydrous fluid, which would have encouraged actinolite replacement of pyroxene and deposition of actinolite in the fractures.

At a later time, near-surface oxidation generated minor goethite after actinolite.

**SAMPLE : 3. ED102-1 (Weathered Kenella Gneiss, Earea Dam Goldfield, SA)**

**SECTION NO : ED102**

**HAND SPECIMEN :** The rock chip sample represents a medium-grained massive felsic granitoid rock, composed of pale pink hematite-stained feldspar, translucent grey quartz, and white feldspar. One fragment appears to contain more abundant dark waxy quartz compared with the other fragments.

**ROCK NAME : Weathered, partly retrogressed, biotite granitoid**

**PETROGRAPHY :**

A visual estimate of the modal mineral abundances gives the following:

Mineral	Vol %	Origin
Plagioclase	47	Relict igneous / ?metamorphic
Quartz	35	Relict igneous / metamorphic
Biotite (incl. goethite)	5	?Relict igneous / ?metamorphic / weath'g
Muscovite (incl. sericite)	10	Retrogressive metamorphic
Zircon	Tr	?Relict clastic / ?igneous
Anatase	Tr	?Metamorphic
Goethite/hematite	2	Weathering

In thin section, this sample displays a massive coarse-grained granitoid texture, modified by metamorphic recrystallisation and replacement, and subsequent weathering overprint.

Plagioclase is abundant, occurring as blocky subhedral prisms, anhedral grains, and granular aggregates. They display typical polysynthetic twinning. Local small grains of myrmekite (intergrown plagioclase and vermiform quartz) are observed in the granular aggregates, or at margins of quartz-muscovite altered ?K-feldspar grain sites. All plagioclase grains display partial replacement by small flecks of white mica ('sericite').

Quartz is abundant, forming sutured monomineralic mosaics that represent partial recrystallisation of precursor large anhedral grains of primary origin. Small fluid inclusions pervade the quartz in minor numbers: most appear to be two-phase types, but some contain a small vapour bubble in clear liquid (probably aqueous compositions) whereas others are filled by a dark fluid bubble (probably CO<sub>2</sub>-rich in composition).

Biotite was abundant, forming randomly oriented plates and subradiating aggregates scattered through the rock. They appear to have formed between the plagioclase grains and aggregates. All of the biotite has suffered turbid discolouration by poorly crystallised orange-brown clays and iron oxide of weathering origin.

White mica occurs in different forms:

- Some occurs as tiny randomly oriented flakes ('sericite') distributed through all plagioclase grains.
- Some white mica occurs as randomly oriented larger well-shaped plates ('muscovite') which are concentrated with quartz in anhedral grain sites which may have been K-feldspar. Rare relict K-feldspar is observed in some of these sites.



Zircon is rare, occurring as ovoid inclusions in some plagioclase grains. The zircon appears to contain ovoid core, with a thin ovoid overgrowth. A complex origin is likely for these cored zircon grains.

Anatase occurs as uncommon ragged grains and small aggregates, with typical blue to blue-green colours, high relief, and very strong birefringence.

Cryptocrystalline iron oxide minerals (goethite, hematite) occur as very fine specks and loose aggregates that are irregularly distributed through the rock, locally in the plagioclase grains.

## INTERPRETATION :

This sample is interpreted to have formed as a massive granitoid igneous rock, originally composed of plagioclase, quartz, K-feldspar, biotite and trace zircon. A possible crustal origin (ie S-type granitoid) is inferred from the presence of biotite as the sole ferromagnesian phase (therefore peraluminous), apparent lack of magnetite (therefore relatively reduced magma composition), and possible presence of inherited zircon (relict clastic zircon as cores in thinly rimmed zircon grains).

The granitoid rock is considered to have suffered a metamorphic overprint event, which caused replacement of K-feldspar by quartz + muscovite, and partial replacement of plagioclase by sericite. It is possible that primary biotite may have suffered partial recrystallisation during this event, but these details have been obscured by subsequent weathering which generated turbid clays and iron oxides in the biotite and elsewhere through the rock. The small fluid inclusions that pervade the partly-recrystallised quartz most probably were trapped during this retrogressive event, and therefore are likely to represent the retrogressive metamorphic fluid.

**SAMPLE : 4. ED21-1 (Calcrete with mafic intrusive, Earea Dam Goldfield, SA)**

**SECTION NO : ED21-1**

**HAND SPECIMEN :** The rock sample is composed of an angular cm-sized dark green mafic rock fragment enclosed in a fine-grained sandy matrix dominated by pale pinkish cream calcite.

The dark green fragment responds weakly to the hand magnet, suggesting minor magnetite is present.

The pale pinkish cream calcite matrix effervesces strongly in reaction with dilute HCl, confirming the abundance of calcite.

**ROCK NAMES : Weakly weathered, partly retrogressed, pyroxene-hornblende granulite**

**Sandy calcrete**

**PETROGRAPHY :**

A visual estimate of the modal mineral abundances gives the following:

Mineral	Vol %	Origin
<i>Weakly weathered, partly retrogressed, pyroxene-hornblende granulite</i>		
Plagioclase	50	Metamorphic 1
Hornblende	20	Metamorphic 1
Opagues (include. magnetite)	2	Metamorphic 1
Actinolite	25	Metamorphic 2 / fracture filling 2
Opagues (?magnetite)	Tr	Metamorphic 2
Goethite	2	Weathering
<i>Sandy calcrete</i>		
Quartz	5	Crystal fragments
Feldspar	1	Crystal fragments
Lithics (plag, quartz, K-feld)	2	Lithic fragments
Ferruginous clay	15	Weathering 1
Calcite	75	Weathering 2
Opaline silica (incl. chalcedony)	2	Weathering 3

In thin section, this sample displays a granoblastic metamorphic texture in the large lithic fragment, and a matrix-supported clastic texture in calcrete.

*Weakly weathered, partly retrogressed, pyroxene-hornblende granulite* displays an equigranular massive granoblastic metamorphic texture defined by small equant anhedral grains of plagioclase, pleochroic dark green hornblende, moderately abundant ferromagnesian grains (pyroxene) replaced by pleochroic pale green actinolite and minor small opaques. Larger anhedral opaque grains form part of the granoblastic assemblage, and are distributed more-or-less uniformly through the rock: the weak magnetic response of the hand sample suggests that at least some magnetite is present in the opaques.

Thin brittle fractures form conjugate sets which are filled by pale green actinolite.

Cryptocrystalline reddish brown goethite occurs as dense turbid replacements in some of the actinolite-altered ferromagnesian grains, near active weathering margins of the fragment.

*Sandy calcrete* contains small angular crystal fragments (mainly quartz, some feldspar) and uncommon larger angular fragments of felsic crystalline rock (plagioclase, quartz, K-feldspar), irregularly distributed through a fine-grained matrix. In places, very fine-grained orange-brown ferruginous clay forms thin coatings on some clastic particles, and also forms larger coherent fragments that contain small angular crystal fragments.

Calcite is moderately abundant, forming a very fine-grained cement that binds the crystal fragments and ferruginous clay fragments.

A small amount of water-clear colourless opaline silica thinly lines pore spaces in the calcite cement, and local small angular pore-space fillings display fibrous textures of chalcedonic silica.

#### INTERPRETATION :

This sample represents a near-surface calcrete which formed through different stages:

1. Protolith fragments were transported in the surficial environment. The fragments included felsic crystalline rock and crystal fragments derived from it, and mafic granulite.
2. Ferruginous clay was deposited as a cement enclosing the fragments.
3. Calcite formed a fine cement enclosing the fragments.
4. A small amount of low-temperature silica (opaline silica, chalcedony) formed as thin linings in pores in the calcrete.

**SAMPLE : 5. ED17-1 (Kenella Gneiss, Earea Dam Goldfield, SA)**

**SECTION NO : ED17-1**

**HAND SPECIMEN :** The rock sample represents a medium-grained felsic granitoid rock, in which indistinctly aligned waxy grey quartz grains and blebs define a foliation in abundant granular feldspar with pale pinkish pervasive hematitic stain.

**ROCK NAME : Weakly weathered foliated leuco-granitoid (biotite quartz monzonite)**

**PETROGRAPHY :**

A visual estimate of the modal mineral abundances gives the following:

Mineral	Vol %	Origin
Plagioclase	42	Igneous
K-feldspar (orthoclase microperthite)	20	Igneous
Quartz	35	Igneous
Biotite	<1	Igneous
Opagues (incl. leucoxene)	Tr	Igneous / weathering
Zircon	Tr	Igneous/ ?relict primary
Goethite/hematite	1	Weathering

In thin section, this sample displays a medium-grained xenomorphic granitoid texture with indistinct foliation, modified by weak pervasive weathering.

Plagioclase is abundant, occurring as anhedral grains ~0.2-2.0 mm in size. They tend to be concentrated in granular aggregates weakly elongated in the trace of a structure (foliation) through the rock. All of the plagioclase grains display incipient clouding from minute phyllosilicate flecks (?illitic clay) and minor tiny iron oxide specks and patches. In places, some anhedral small plagioclase grains contain vermiform intergrowths of quartz (myrmekite).

K-feldspar is moderately abundant, forming anhedral grains ~1-2 mm in size that tend to be larger than most of the plagioclase grains. Most display oriented wispy blebs of exsolved albite, that is, the K-feldspar grains are orthoclase microperthite.

Quartz is moderately abundant, forming large ovoid interlinked patches of sutured granular mosaics. They appear to represent partly-recrystallised primary coarse grained quartz. Abundant fluid inclusions are distributed throughout the quartz grains, and also tend to be concentrated along thin sealed microcracks which transect the sutured grain margins and therefore are post-recrystallisation. Some are composed of a small vapour bubble in clear liquid (ie aqueous compositions), whereas others are filled partly or entirely by a dark bubble (probably H<sub>2</sub>O-CO<sub>2</sub> compositions).

Biotite occurs in minor amount as uncommon flakes pleochroic from dark reddish brown to pale yellow. Most have suffered partial colour modification in response to weathering.

Opagues occur in trace amount as small blocky grains and small cusped grains in granular plagioclase aggregates. Their identification remains uncertain in the absence of reflected light observations.

Zircon is rare, forming ovoid to stumpy subhedral grains, in quartz and also in plagioclase.

## INTERPRETATION :

This sample represents a leuco-granitoid rock of inferred igneous origin. The anhedral grain shapes are consistent with formation as a felsic segregation band or injection vein in a high-grade metamorphic terrain. The indistinct foliation, as defined by aligned elongated quartz grains, supports development in a high-grade regional metamorphic terrain. The primary rock was composed of plagioclase, quartz, K-feldspar, minor biotite and opaques, and trace zircon.

It is considered likely that the rock suffered a retrogressive event which is not evident in the present mineralogy. It might have been responsible for the partial recrystallisation of the quartz, and it is most likely responsible for the entrapment of abundant fluid inclusions in the recrystallised quartz.

At a later time after uplift and erosion, the rock suffered minor pervasive weathering, which generated minor fine iron oxides pervasively through the rock.

**SAMPLE : 6. ED241-1 (Hardpan, Earea Dam Goldfield, SA)**

**SECTION NO : ED241-1**

**HAND SPECIMEN :** The sample is composed of angular competent but porous rock fragments, all of which represent massive reddish brown ferricrete which contains moderately abundant small paler and darker fragments of millimetre size. Small void spaces pervade the somewhat porous rock.

**ROCK NAME : Sandy ferruginous claycrete**

**PETROGRAPHY :**

A visual estimate of the modal mineral abundances gives the following:

Mineral	Vol %	Origin
Quartz	42	Crystal fragments
K-feldspar	10	Crystal fragments
Plagioclase	5	Crystal fragments
Hornblende	Tr	Crystal fragments
Opakes	Tr	Crystal fragments
Lithics (quartz, plag, K-feld)	2	Lithic fragments
Ferruginous clay	30	Weathering
Voids	10	Remnant interparticle pores

In thin section, this sample displays a framework-supported arenaceous clastic sedimentary texture, with closely-packed crystal and minor lithic fragments firmly cemented in ferruginous clay.

Crystal fragments are abundant. Angular clear quartz fragments are mostly ~0.05-0.2 mm in size, but some range up to ~0.4 mm. Similarly sized angular fragments of twinned plagioclase and untwinned K-feldspar (orthoclase microperthite) are less common. Pleochroic green hornblende grains are uncommon but range widely in size (one is ~0.4 mm, others <0.1 mm). Opakes occur as uncommon grains.

Lithic fragments are present in minor amount. Some are quite large (~2-3 mm), and represent felsic crystalline rock of granitoid composition. A single fragment composed of opakes and hornblende appears to represent a mafic granulite.

Much of the rock is composed of very fine-grained orange-yellow ferruginous clay materials which tend to form discontinuous thinly layered fillings between the crystal and lithic fragments. Commonly, the laminated clay fillings progress into void spaces which represent unfilled remnant interparticle pores.

**INTERPRETATION :**

This sample represents poorly sorted angular surficial detrital materials derived from felsic crystalline rock and mafic granulite. The crystal fragments represent those two rock types, and therefore include quartz, plagioclase, K-feldspar, minor opakes and hornblende. Uncommon lithic fragments of felsic crystalline rock and mafic granulite are present in the mainly crystal detritus.

Circulation of surficial meteoric waters resulted in cementation of the detrital components by ferruginous clay material. A significant proportion of the primary interparticle pore space remained unfilled, resulting in a somewhat porous ferruginous sandy rock.



**SAMPLE : 7. ED95-1 (Hematite and quartz, Earea Dam Goldfield, SA)**

**SECTION NO : ED95-1** (Both a thin section and a polished block were provided. A combined petrographic and mineragraphic description is therefore provided below).

**HAND SPECIMEN :** The rock sample represents a rock fragment dominated by massive milky white vein quartz and abundant fine-grained patches of metallic grey hematite (dark red streak).

**ROCK NAMES : Oxidised quartz-sulphide(-gold) vein**

**High-intensity phyllic (quartz-sericite) altered host rock**

**PETROGRAPHY AND MINERAGRAPHY:**

A visual estimate of the modal mineral abundances gives the following:

Mineral	Vol %	Origin
<i>Oxidised quartz-sulphide(-gold) vein</i>		
Quartz	76	Vein filling
Biotite	2	Relict vein filling (partly oxidised)
Pyrite	Tr	Relict vein filling
Native gold	Tr	Vein filling
Hematite (massive specular)	20	Oxidation of ?sulphide (weathering)
Clays	<1	Weathering / fracture fillings
<i>High-intensity phyllic (quartz-sericite) altered host rock</i>		
Quartz	70	Alteration
Sericite	30	Alteration
Goethite	Tr	Weathering

In thin section and polished block, this sample displays a coarse-grained vein texture modified by partial recrystallisation and weathering, and an indeterminate host rock (?quartzo-feldspathic) modified by strong pervasive alteration.

*Oxidised quartz-sulphide(-gold) vein* retains its primary coarse-grained space-filling vein texture despite subsequent modification in different events.

Quartz is abundant, and occurs in two forms:

- i) Some occurs as large anhedral grains up to several millimetres in size. This represents relict primary coarse-grained vein quartz. Tiny fluid inclusions (mostly <2 µm in size, some up to ~5 µm) pervade the quartz in large numbers, but are too small for useful petrographic observations. Larger inclusions appear to represent two-phase types that include both aqueous (small vapour bubble in clear liquid) and CO<sub>2</sub>-rich (large dark fluid bubble) types.
- ii) Much quartz occurs as fine-grained sutured mosaics which pervade and enclose the relict larger primary grains described above. These sutured mosaics clearly represent recrystallised precursor coarse-grained vein quartz: fluid inclusions are absent from these water-clear mosaics.

Hematite is abundant, occurring as uniformly fine-grained microgranular mosaics which occupy large ragged patches distributed somewhat irregularly through the rock. No relict precursor minerals are preserved in the hematite patches, but it may have been sulphide (see next).

Pyrite is observed as a single small cubic crystal enclosed in vein quartz. It has suffered partial replacement from margins inwards by goethite.

Phyllosilicate flakes are intergrown with hematite aggregates at their contacts with quartz. The flakes are inferred to represent biotite, now severely modified by pervasive discolouration in response to weathering. A small amount of clay material occurs as cryptocrystalline massive pale patches associated with the altered phyllosilicate flakes and hematite.

Native gold has been observed in rare small grains:

- i) One small equant grain ~50  $\mu\text{m}$  in size occurs within vein quartz. It clearly represents part of the vein-filling assemblage. The bright golden yellow grain appears to be of relatively high fineness (ie low Ag content).
- ii) One small ragged grain occurs within a small hematite aggregate. It remains uncertain whether this grain represents a relict primary grain, or remobilised gold as part of the weathering overprint.

*High-intensity phyllic (quartz-sericite) altered host rock* occurs at margins of the vein. Quartz forms sutured mosaics, and sericite tends to be concentrated in fine-grained aggregates. Goethite is concentrated along some thin irregular fractures.

## INTERPRETATION :

The mineralogy and microtextures of this sample are interpreted in the following evolution, from earliest to latest event:

### 1. Generation of host rock

A host rock, possibly of quartzo-feldspathic composition, developed as part of the country rock association. No primary minerals or textures of the rock are preserved, but it might have been of quartzo-feldspathic composition, as inferred from the subsequent alteration assemblage (see next).

### 2. Fracturing, veining and wall rock alteration

The host rock suffered fracturing and invasion by hydrothermal fluid. This resulted in filling of the open fractures by space-filling assemblages of quartz + sulphide (including pyrite) + minor biotite + trace native gold. Abundant fluid inclusions were trapped in the vein quartz, and therefore represent the mineralising fluid. Marginal to the vein, host rock suffered complete pervasive replacement by the phyllic assemblage of quartz + sericite.

### 3. Mild deformation

The rock body suffered mild deformation, resulting in partial recrystallisation of vein quartz to finer-grained sutured mosaics in which the precursor fluid inclusions were destroyed. This event might represent waning stages of event 2, or possibly a later distinct event.

### 4. Uplift, erosion and weathering

After uplift and erosion, the rock body suffered invasion by circulating near-surface meteoric waters. This generated abundant fine-grained hematite after ?sulphide, and also generated minor goethite and clays.

**SAMPLE : 8. TE104 (Calcrete from dune, Earea Dam Goldfield, SA)**

**SECTION NO : TE104**

**HAND SPECIMEN :** The coherent but porous sample represents reddish brown sandy ferricrete that is partly mantled by fine-grained pale cream calcite (effervesces strongly in reaction with dilute HCl).

**ROCK NAME : Calcreted sandy ferricrete**

**PETROGRAPHY :**

A visual estimate of the modal mineral abundances gives the following:

Mineral	Vol %	Origin
Quartz	39	Clastic particles
Opaques	Tr	Clastic particles
Rutile	Tr	Clastic particles
Hornblende	Tr	Clastic particles
Ferruginous clay	30	Weathering 1
Calcite	25	Weathering 2
Voids	5	Weathering 2

In thin section, this sample displays a clastic sedimentary texture, with fine cements of two generations.

Quartz is abundant, occurring as angular to rounded crystal fragments of unstrained quartz ~0.1-0.8 mm in size (mostly ~0.2-0.4 mm). They form a framework-supported texture through most of the rock.

Other crystal fragments are rare. Opaques occur as small grains, and rutile forms rare small equant grains of typical high relief and yellow colour. Hornblende occurs as rare small angular grains with typical dark green pleochroism and moderate interference colours.

Ferruginous clay is moderately abundant, forming a fine-grained reddish brown matrix that binds the abundant quartz clasts. The clay tends to be most dense immediately around the clasts, where it forms a thinly laminated matrix. It tends to become less dense away from the clasts, and locally gives way to fine-grained calcite which fills in the interstices. Calcite also occurs abundantly in the weakly laminated mantle, and in indistinct veinlets that pervade the rock. Ragged solution cavities pervade the rock, producing a somewhat porous texture.

**INTERPRETATION :**

This sample represents sandy detrital materials (quartz >> others including opaques, rutile, hornblende). Transport and abrasion in the surficial environment resulted in rounding of larger quartz grains.

Cementation commenced with deposition of thinly laminated ferruginous clay materials around each particle, resulting in a firmly bound deposit. Subsequent deposition of fine-grained calcite continued the cementation process, filling remnant pores and thin diffuse veinlets, and forming a fine-grained rind on the sample.

## **APPENDIX 2**

**Disc containing text of report, tabulated data, raw data, photographs, annotated XRD spectra and GIS**